The YdiU Domain Modulates Bacterial Stress Signaling through UMPylation

Yinlong Yang[1,2,#], Yingying Yue[1,#], Cuiling Li[1,#], Nannan Song[1,#], Zenglin Yuan[3], Yan Wang[4], Yue Ma[1,2], Hui Li[1,2], Fengyu Zhang[3], Weiwei Wang[1], Haihong Jia[1], Peng Li[1], Xiaobing Li[1], Hongjie Dong[3], Lichuan Gu[3,*] and Bingqing Li[1,*]

[1] Key Laboratory of Rare and Uncommon Diseases, Department of Microbiology, Institute of Basic Medicine, Shandong First Medical University & Shandong Academy of Medical Sciences, Jinan 250062, China.

[2] School of Medicine and Life Sciences, University of Jinan-Shandong Academy of Medical Sciences, Jinan 250062, China.

[3] State Key Laboratory of Microbial Technology, School of Life Sciences, Shandong University, Qingdao, 266237, China.

[4] College of Marine Life Sciences, MOE Key Laboratory of Marine Genetics and Breeding, Ocean University of China, Qingdao, 266003, China.

# These authors contributed equally.

*To whom correspondence should be addressed.

Dr. Bingqing Li, Tel. 86-531-82919938; Fax:86-531-82919930; E-mail: bingqingsdu@163.com

Dr. Lichuan Gu, Tel. 86-532-58632443; Fax:86-532-58632443; E-mail: lcgu@sdu.edu.cn

Running title: YdiU-mediated UMPylation

ABSTRACT

Sensing stressful conditions and adjusting metabolism to adapt to the environment is essential for bacteria to survive in changeable situations. Here, we discover a new stress-induced protein YdiU, demonstrate a role of YdiU in bacterial heat stress resistance and identify YdiU as an enzyme that catalyzes the covalent attachment of uridine 5'-monophosphate to a tyrosine or histidine residue of bacterial proteins—a novel modification defined as UMPylation. Consistent with the recent finding that YdiU acts as an AMPylator, we further reveal that self-AMPylation of YdiU negatively regulates its UMPylation activity. The detailed molecular mechanism of YdiU-mediated UMPylation and substrate selectivity are proposed based on the determination of the crystal structures of Apo-YdiU, YdiU-ATP and YdiU-AMP complexes and a molecular dynamics simulation model of the YdiU-UTP complex. Biochemical data show that UMPylation of chaperones mediated by YdiU prevents them from binding either downstream co-factors or their substrates, thereby impairing their function. Interestingly, UMPylation mediated by YdiU also promotes the degradation of chaperones. *In vivo* data show that YdiU effectively protects *Salmonella* from heat injury by preventing stress-induced ATP depletion and UMPylation occurs in response to heat stress in a YdiU-dependent manner. Together, our results illuminate new biological functions of the YdiU domain family, highlight the importance of UMPylation in bacterial signal transduction, and reveal a potential mechanism by which bacteria adapt to different levels of stressful environment.

KEYWORDS: Post translational modification, UMPylation, AMPylation, the YdiU domain, Chaperones, Bacterial themo-resistence

INTRODUCTION

Bacteria survive in a changeable environment and have evolved myriad mechanisms to sense and respond to stress conditions. The most well-known strategy is to change gene expression in response to environmental variation[1]. Transcription factors or alternative sigma factors are activated under stress conditions, and bind to their target genes to activate or inhibit transcription of the regulated genes[2, 3]. Post-translational modifications (PTMs) of proteins also play an important role in the regulation of stress response. Bacterial two-component signal transduction systems, consist of a histidine kinase and a response regulator, and regulate cellular physiology

through a series of phosphorylation events[4, 5]. Protein acetylation modulates many cellular processes of bacteria such as metabolism, bacterial chemotaxis and DNA replication response to different environments[6, 7, 8]. Additionally, other modifications such as carbonylation, nitration, N-myristoylation, phospholipid, glycosylation, ADP-ribosylation, and AMPylation have been detected in bacteria, however, the targets and mechanism of those modifications and their role in stress resistance remain largely unknown[9, 10, 11, 12].

The YdiU (also known as SelO or UPF0061) domain is a pseudokinase domain that is widely found in three kingdoms of life and is highly conserved from *E.coli* to human (43% in full-length sequence identity)[13]. Over 15,000 proteins contain a predicted YdiU domain (InterPro Database; IPR003846; http://www.ebi.ac.uk/interpro/index.html). However, the *in vivo* and *in vitro* function of the YdiU domain has not been characterized until recently, making it one of "the top ten most-attractive unknown domains"[14, 15]. Most species of bacteria contain a single YdiU domain protein, and previous transcriptomic data showed an increase in YdiU during the recovery stage after heat shock, hydrostatic pressure, and osmotic stress implying a relationship between YdiU and bacterial stress resistance[16, 17, 18]. Most recently, Sreelatha *etal* reported a role of YdiU in redox homeostasis and identified YdiU as an AMPylator that transfers AMP from ATP to Ser, Thr, and Tyr residues on protein substrates[19]. In addition to auto-AMPylation, two proteins involved in redox homeostasis were found to be AMPylated substrates of YdiU. The discovery by Sreelatha *et al.* that YdiU acts as an enzyme that mediates protein modification significantly advances investigation into the functions of YdiU family proteins. However, how AMPyaltion regulates the activities of substrates and whether YdiU modifies other protein substrates and functions as part of other responses requires further investigation.

In this study, we demonstrated a role of YdiU in bacterial stress resistance and discovered an unexpected activity of YdiU to catalyze UMP-modification of bacterial chaperones. Chaperones play an important role under stress conditions by repairing misfolded proteins. In bacterial chaperone networks, GroEL and DnaK function as the central hubs, with activity contributions from other proteins, such as HtpG and ClpB[20, 21]. Our data showed indubitably that all these chaperones, GroEL, DnaK, HtpG, and ClpB, could be UMPylated by YdiU *in vivo* and *in vitro*. Interestingly, YdiU preferred UTP over ATP as co-substrate and the UMPylation activity of YdiU was inhibited by self-AMPylation sensing the intracellular level of ATP. The catalytic and substrate selectivity mechanism of YdiU-mediated NMPylation are proposed by determining the

crystal structure of Apo-YdiU, YdiU-ATP and YdiU-AMP complexes and structural model of YdiU-UTP obtained by molecular dynamics simulation. Further, we revealed that the UMPylation of chaperones by YdiU prevented them from binding either downstream co-factors or their substrates. Not only that, UMPylation of chaperones mediated by YdiU was proved to promote their degradation. *In vivo* data show that *Salmonella* benefits from YdiU-mediated UMPylation under severe heat injury and UMPylation occurs in response to heat stress in a YdiU-dependent manner. In conclusion, this work extends our knowledge of YdiU domain, highlights the importance of protein UMPylation in bacterial signal transduction and reveals a novel mechanism by which bacteria modulate chaperone's activity and degradation by post-translational modification.

RESULTS

The Expression of YdiU is Stress-dependent in *Salmonella*.

To investigate the conditions under which *Salmonella* YdiU is expressed, the mRNA and protein levels of YdiU in *Salmonella* cultured under different conditions were quantified by q-PCR and western blot (Fig.1a, b). Interestingly, YdiU was barely expressed when *Salmonella* was cultured in Luria-Bertani medium at 37°C (normal laboratory growth condition), but surged to high level under multiple stress conditions such as nutritional deficiency, H_2O_2 stress, and acid stress. Remarkably, the level of YdiU rose observably after heat shock and accumulated as the increase of heat time (Fig.1c, d). The fact that stress conditions significantly elevate expression of YdiU suggests YdiU may play a role in the survival of *Salmonella* under stress conditions.

YdiU Protects *Salmonella* form Acute Heat Injury.

To explore the function of YdiU, we constructed a YdiU knockout strain of *Salmonella* (ΔYdiU). The ability of thermal resistance in wild-type *Salmonella* and ΔYdiU strain was determined (Fig.2). When *Salmonella* was treated at 55 °C for only 1 min, no significant difference was observed between WT strain and the ΔYdiU strain. Longer time of heat treatment led to more prominent difference in the survival rate between these two strains. Compared with the WT strain, the ΔYdiU strain following long time heat treatment exhibited significantly reduced survival rate, suggesting that YdiU protects *Salmonella* against heat-induced cell death especially in acute heat stress.

UMPylated Proteins Identified in YdiU-expressing *Salmonella*.

To explore the function of YdiU, an expression plasmid of YdiU was transformed into the ΔYdiU strain to generate a strain that persistently expressed YdiU (pYdiU). The production of YdiU in the pYdiU strain with different concentrations of inducer L-arabinose was determined (Supplementary Fig.S1). In Luria-Bertani medium with 0.1% L-arabinose, the amount of YdiU in pYdiU was approximately equivalent to the one of wild type *Salmonella* under stress conditions. Therefore, the ΔYdiU and pYdiU strains cultured in LB medium with 0.1% L-arabinose were used to study the phenotype of *Salmonella* in the presence or absence of YdiU. Mass spectrometry-based proteomic analysis was performed using ΔYdiU and pYdiU strains. Surprisingly, only a few proteins showed a more than 50% change in expression. Nevertheless, when we analyzed protein modifications using ProteinPilot (a software that allows extensive search for all identified modifications), fifty-six peptides covalently modified with an uridine 5'-monophosphate (UMP) molecule were detected in YdiU-expressing *Salmonella* (Supplementary Table S1). UMPylated peptides were mapped to forty-six different *Salmonella* proteins involved in multiple life activities (Supplementary Fig.S2a, b and Supplementary Table S2). Analysis of the primary sequences of UMPylated peptides reveals some obvious common characteristics (Supplementary Fig.S2c, d): i). UMPylation was observed only on tyrosine or histidine residues; ii). Near most of UMPylation sites (41/56), there is one or more negatively charged amino acids (Asp or Glu); iii). Hydrophobic amino acids (Tyr, Trp, Phe, Ile, Val, and Met) were enriched around the UMPylation sites.

Previously, UMPylation was only observed in glutamine synthetase, in which the synthesis rate of glutamine was modulated by self-modification between subunits[22]. Given that the YdiU domain includes a protein kinase fold and a hypothetical nucleotide binding site, we hypothesized that YdiU could act as an UMPylator (an enzyme that catalyzes UMPylation, Fig.3c). Analysis of the UMPylated proteins in YdiU-expressing *Salmonella* suggests that YdiU could catalyze self-UMPylation (Fig.3a and Supplementary Fig.S3a). Other substrates of YdiU are key players in many vital activities, revealing a potentially extensive regulatory role of YdiU and UMPylation (Supplementary Fig.S2a). Remarkably, all major chaperones (GroEL, DnaK, HtpG, and ClpB) of bacteria were UMPylated by YdiU *in vivo* (Fig.3b and Supplementary Fig.S3b-d). Chaperones are essential for bacteria to survive under heat stress conditions by repairing misfolded proteins, so the regulation of chaperones by YdiU through UMPylation may

associate with the thermal resistance of *Salmonella* under heat stress. Thus, chaperones were focused on and examined in more detailed in this study.

YdiU Mediates Self-UMPylation and UMPylation of Chaperones *in vitro*.

To further confirm the function of YdiU as an UMPylator, we purified full-length *E.coli* YdiU (478aa, $YdiU^{fl}$) and a truncated version lacking the C-terminal three amino acids ($YdiU^{475}$). The purified proteins were tested using *in vitro* assays with α^{32}P-UTP in the presence of different divalent metal ions (Fig.3d). Interestingly, ^{32}P-UMP-YdiU products were observed with buffers containing Mn^{2+}. *Salmonella* increases the absorption of manganese in response to multiple stress signals[23, 24]. The activation of UMPylation activity of YdiU by manganese suggests a regulatory mechanism of enzyme activity that utilizes metal ion. Subsequent *in vitro* UMPylation assays of chaperones were performed using Mn^{2+} as an activator and α^{32}P-UTP or biotin-16-UTP as the UMP donor respectively (Fig.3e, f). The assay results clearly showed that all those chaperones could be UMPylated by YdiU *in vitro*. Additionally, the *in vitro* UMPylation levels of GroEL, DnaK, and HtpG catalyzed by YdiU were high while that of ClpB was observed in a more limited extent suggesting the differences of the UMPylation activity mediated by YdiU with different substrates.

YdiU Can Use Both UTP and ATP as Co-substrate.

Our data showed that YdiU catalyzed both self-UMPylation and substrate UMPylation *in vivo* and *in vitro*. Recently, Sreelatha *etal* reported YdiU act as an AMPylator and two AMPylated proteins (GrxA and SucA) involved in redox homeostasis[19]. To further investigate the selectivity of YdiU for ATP and UTP, a biotin-labeled assay utilizing biotin-16-UTP or biotin-17-ATP as NMP donors was developed (Fig.4a). The K_m values of YdiU using UTP or ATP as the substrate were estimated by monitoring UMP-YdiU and AMP-YdiU production. The K_m value of YdiU for UTP as substrate was about 0.6 μM, lower than that for ATP, 1.7 μM. Furthermore, the AMPylation and UMPylation of GroEL catalyzed by YdiU were assayed (Fig.4b). Strikingly, GroEL could be AMPylated by YdiU *in vitro,* but to a much lower extent (≈1/5) than the observed UMPylation. We also purified GrxA, the AMPylated substrate identified by Sreelatha *etal*. However, we did not detect either AMPylation or UMPylation of GrxA in our reaction system, we are unable to determine if this AMPylated substrate can also be UMPylated by YdiU. Next, the interaction between non-degradable analogues of UTP (UMPNPP) or ATP (AMPNPP)

and YdiU was detected by biolayer interferometry (BLI). The obtained dissociation constant (K_d) values for YdiU and UMPNPP interaction was ~17 μM and that of AMPNPP was ~67 μM in buffer with Mg^{2+} (Supplementary Table S3). In the absence of Mg^{2+}, the interaction between YdiU and AMPNPP was too weak to be detected and that of YdiU-UMPNPP remained ~20 μM suggesting that Mg^{2+} is more important in YdiU-ATP interaction than YdiU-UTP interaction (Fig.4c, d). Isothermal titration calorimetry (ITC) assay was used to detect the change of heat after YdiU binding to UMPNPP or AMPNPP. The binding of YdiU to UMPNPP was an exothermic reaction, but no signal was detected for AMPNPP (Fig.4e, f). Together, our data suggested YdiU is able to use either UTP or ATP as substrate *in vitro*, but that UTP was the preferred substrate.

Self-AMPylation Inhibits the UMPylation Activity of YdiU.

Although the above data demonstrated that YdiU preferred UTP over ATP *in vitro*, the fact that UTP is present at lower concentration than ATP implies that YdiU will utilize ATP and remain in a self-AMPylated state under normal conditions[25]. Sreelatha *etal* mapped the major self-AMPylation sites of *E.coli* YdiU to its C-terminal region, Ser477 and Ser478[19]. Consistent with their result, our data showed that $YdiU^{475}$ was not able to mediate self-AMPylaton but showed greater activity to AMPylate substrates than that of full-length YdiU (Fig.4b). To investigate the effect of self-AMPylation on YdiU-mediated substrates UMPylation, another biotin-based assay was performed. Firstly, $YdiU^{fl}$ or $YdiU^{475}$ was AMPylated *in vitro* and purified. Then the activities of AMPylated and non-AMPylated YdiU to UMPylate GroEL were detected. The AMPylated $YdiU^{fl}$ lost the ability to UMPylate GroEL while the AMPylated $YdiU^{475}$ showed a similar activities with the non-AMPylated $YdiU^{475}$ (Fig.5), suggesting self-AMPylation of YdiU on its Ser 477 and/or Ser 478 significantly inhibited the UMPylation activity of YdiU. Thus, the UMPylation of substrates mediated by YdiU might be modulated through self-AMPylation in response to the cellular level of ATP.

Structural Insight into the Catalytic Mechanism of YdiU-mediated NMPylation.

To further investigate the mechanism of YdiU-associated UMPylation/AMPylation, we tried to obtain crystal structures of YdiU. The crystal structure of *E.coli* YdiU-AMPPNP was solved using selenium single wavelength anomalous diffraction at 2.0 Å resolution and structures of Apo-YdiU and YdiU-AMP-PPi were solved by the molecular replacement approach based on the

structure of YdiU-AMPPNP. The overall structure of YdiU exhibits a novel fold in which the catalysis domain is stabilized by the C-terminal regulatory domain, which looks like a big "clamp" (Fig.6a, b). The AMPPNP or AMP/PNP molecule is clearly defined in the corresponding electron density maps (Fig.6c, d). The nucleic acid binding site is located in a cleft at the interface between the N-lobe and C-lobe of the catalysis domain. The ATP analog is positioned with Mg^{2+} in the active site via a novel binding mode in which the ɤ-phosphate is deeply buried in a pocket with the purine ring located outside the pocket. A similar structure of *P. syringae* YdiU in complex with AMPPNP, Mg^{2+} and Ca^{2+} was reported recently by Sreelatha *etal*. Despite sequence identity of 48%, the catalytic domain of *E.coli* YdiU displays a very similar conformation to that of *P. syringae* YdiU[19]. The basic group of AMPPNP is fixed through two hydrogen-bond interactions with Asp119 and Gly120 (Fig.6f). An extensive network of interactions orients the β and ɤ phosphates with Arg87, Lys107, Arg170 and Arg177. Two Mg^{2+} coordinate with phosphate groups, and Asp 256 and Asn 247 clamp the AMPPNP to facilitate ATP hydrolysis (Fig.6f). Notably, before ATP binding, as shown in the structure of Apo-YdiU, the orientations of Asp256, Lys107 and Arg87 are completely different (Fig.6e and Supplementary Fig.S4a). In the absence of the nucleotide and ions, Asp256 interacts with Arg170 and Arg177 while Arg87 interacts with Asp119 via electrostatic interaction (Fig.6e). Superposition of the YdiU-AMPPNP and YdiU-AMP structures reveals that the purine ring and nucleic sugar adopt the same position in the active center, however, the phosphate of AMP is displaced from the α-phosphate of ATP and instead is coordinated with Gln75, Asn244, and Asn247 in the YdiU-AMP structure (Supplementary Fig.S4b and Fig.6g). Notably, residues involved in the active site are strictly conserved from bacteria to human, suggesting a uniform mechanism for YdiU homologues (Fig.6h and Supplementary Fig.S5). Based on the structures, a general model for the catalysis mechanism of YdiU-mediated NMPylation is proposed in which the strictly conserved Asp 246 acts as the general base and activates the oxygen of the hydroxyl group from Tyr or the nitrogen from His for nucleophilic attack (Fig.6i). The exact role of these residues was investigated further by mutagenesis. Most mutations of residues in the active center completely abolished enzyme activities (Fig.6j). Intriguingly, when Asp119, the major residue to immobilize the purine ring of ATP, was replaced with Alanine, the UMPylated activity was reduced but not completely abolished suggesting that Asp119 might play a secondary role in UTP binding and UMPylation.

Structure Basis for the Nucleiotide Preference of YdiU.

Biochemical experiments suggested that YdiU preferred UTP over ATP as a donor substrate. Regrettably, we were unable to obtain the structure of YdiU-UTP due to poor diffraction of crystals. To investigate the mechanisms underlying the nucleotide selectivity of YdiU, we modeled the YdiU-UTP complex using molecular docking based on the crystal structure of Apo-YdiU. The docking result positioned UTP in the same cavity of YdiU as ATP (Fig.7a). Superposition of YdiU-UTP with the crystal structure of YdiU-ATP shows that two conserved loops responsible for Basic Fixation (BF motif 1 and BF motif 2) undergo arresting transformations. Compared with ATP forming three hydrogen bond interactions of its purine ring with YdiU, four hydrogen bonds were predicted to form between the pyrimidine ring of UTP and YdiU (Fig.7b-e). Additionally, the O5' of UTP provides an extra hydrogen bond interaction with Gln75 of YdiU , which is absent in YdiU-ATP interaction (Fig.7b-e). These observations are consistent with the results of our *in vitro* data showing a stronger binding affinity of YdiU to UTP than to ATP.

Structure-based molecular dynamics simulation of YdiU binding with either UTP or ATP was performed. The obtained convergence parameters suggested that both structures of YdiU-ATP and YdiU-UTP were stable during simulation. The root mean square deviation (RMSD) value and radius of gyration (Rg) value of YdiU-UTP were slightly lower than these of YdiU-ATP implying the structure of YdiU-UTP is more stable than that of YdiU-ATP during simulation (Supplementary Fig.S6). Six hydrogen bonds occurred between YdiU and ATP while seven occurred in YdiU-UTP coinciding with docking result described above. The calculated binding free energy and its main energy items were listed in Supplementary Table S4. Remarkably, the binding energy(ΔG_{bind}) of YdiU-UTP was -25.87 kcal/mol, lower than that of YdiU-ATP, -23.52 kcal/mol, confirming the stronger affinity of YdiU-UTP than YdiU-ATP. Thus, more hydrogen bond interactions of YdiU-UTP than YdiU-ATP stabilize YdiU-UTP structure, thereby lead to the preference of YdiU for UTP over ATP.

Mechanism for Substrate Recognition of YdiU-mediated UMPylation.

Our *in vivo* data suggested that UMPylation can occur on tyrosine or histidine residues and negatively charged and hydrophobic residues enriched around the UMPylation sites. To investigate the mechanism of substrate specificity of YdiU-mediated UMPylation, an UMPylated

Tyr residue and an Asp residue at the -1 position were superimposed in the position of the AMP molecule in the YdiU-AMP-PPi structure. Near the substrate-binding site, a hydrophobic pocket consisting of residues Phe76, Val242 and Tyr281 and electropositive Arg116 came under observation (Supplementary Fig.S7a). The hydrophobicity of this substrate-binding pocket well explains the frequent observation of hydrophobic amino acids around the UMPylation sites. Additionally, the conserved Arg116 might interact with the negative residues of substrate through electrovalent bonds (Supplementary Fig.S7a). Notably, the identified feature in substrate recognition was completely conserved in different species, suggesting a similar substrate selectivity for orthologs of YdiU (Supplementary Fig.S7b). The exact role of these residues was investigated using mutagenesis. Mutants of Thr112, Arg116, Val242, and Tyr 281 abolished the UMPyaltion activities of YdiU and substitutions in Phe76, Ser115 exhibit little change compared with native YdiU (Supplementary Fig.S7c). These observations highlight the importance of Arg116, Val242 and Tyr281 in substrate-binding and catalytic activity of YdiU.

Finally, a model for YdiU-mediated UMPyaltion was established (Supplementary Fig.S8): i). Before UTP binding, the essential residue Asp 256 is blocked by Arg170 and Arg 177; ii). UTP and divalent metal bind to the active site through a series of interactions; iii). The hydrophobic region of the substrate is recognized by the hydrophobic pocket, consisting of Phe76, Val242 and Tyr281. The negatively charged residue near the UMPylation site coordinates with Arg116; iv). Asp246 activates the substrate for nucleophilic attack, the UTP is hydrolyzed, and the UMP moiety of UTP transfers to the Tyr or His residue of substrate.

UMPylation Prevents Chaperones from Binding Substrates or Co-factors.

To determine how UMPylation modulates the function of chaperones, the sites of UMPylation were analyzed further. The UMPylated sites of chaperones were all in close proximity to the regions responsible for substrate/cofactor binding or self-assembly. Tyr199 and Tyr203 of GroEL are localized to the hydrophobic pocket and facilitate both substrate and co-factor GroES binding (Fig.8a). As reported previously, mutagenesis of Tyr199 and Tyr203 completely abolished substrate binding[26, 27]. Tyr199 and Tyr203 of GroEL were further confirmed as the major UMPylation sites by *in vitro* UMPylation assay with GroEL mutants (Fig.8b). Next, the interactions between non-UMPylated GroEL or UMPylated GroEL and human ornithine carbamoyltransferase (OTC, a well-established substrate of GroEL) were monitored using an improved pull-down assay (Supplementary Fig.S9). The results indicated that UMPylation

strongly inhibited the GroEL-substrate interaction (Fig.8c), implying a novel mechanism to inhibit chaperone function. The UMPylation site of HtpG was also located near the substrate-binding cavity, suggesting UMPylation of HtpG could affect its interaction with substrates (Supplementary Fig.S10a)[28]. DnaK requires two cofactors, DnaJ and GrpE, to achieve its chaperone function[29, 30]. Interestingly, the *in vivo* assay identified the modification site of DnaK as Tyr285, which is located at the interface between DnaK and GrpE (Fig.8d). Biolayer interferometry assays were performed and further confirmed that UMPylation interfered with the interaction between DnaK and GrpE (Fig.8e and Supplementary Fig.S11). The activity of ClpB requires assembly into a hexamer[31]. The UMPylated residue Tyr812 of ClpB is positioned at the interface between monomers, suggesting that UMPylation of ClpB might influence hexamer assembly and therefore alter ClpB function (Supplementary Fig.S10b). Overall, the UMPylation by YdiU targets residues in these chaperones that would interfere with their function.

YdiU-mediated UMPylation Promotes the Degradation of Chaperones.

To investigate the detailed mechanism of YdiU-mediated thermal resistance, the expression level of YdiU and DnaK during heat shock repair were analyzed (Fig.9a). *Salmonella* elevates the expression of DnaK less than 5 min after heat, while YdiU starts to express 10 min after heat treatment, reaching its the highest level 45 min after heat treatment. Interestingly, the level of DnaK was observed to be negatively correlated with the quantity of YdiU (Fig.9a). To further determine the relationship of YdiU and chaperones under heat stress, four *Salmonella* strains containing wild-type [32], *ydiU* knockout strain (ΔYdiU), or that strain expressing YdiU (pYdiU) or inactive YdiU mutant D256A (pYdiU D256A) were constructed. Then the levels of chaperones and YdiU of these strains with or without heat treatment were detected by western blot (Fig.9b). Following acute heat treatment (55 ^{o}C for 5 min), the intracellular levels of GroEL and DnaK in ΔYdiU are accumulated significantly. By contrast, the ones in WT and pYdiU strains expressing high level of YdiU did not changed or even reduced after heat treatment (Fig.9c), further suggesting YdiU might regulate the amount of chaperones under acute heat stress. According to the finding that YdiU mediates the UMPylation of chaperones, we hypothesized that the half-life of UMPylated chaperones might be different with unmodified ones, as a result, YdiU will promote the degradation of chaperones through UMPylation. To test this hypothesis, degradation assays of GroEL and DnaK with native YdiU or YdiU D256A mutant were performed (Fig.9d, e). The addition of native YdiU launched the degradation of

both GroEL and DnaK, while the inactive mutant of YdiU did not work. These data suggest that YdiU-mediated UMPylation does accelerate the degradation of chaperones.

YdiU Prevents Stress-induced ATP depletion.

Recovery from heat injury consumes lots of ATP. Under ATP-limited condition, the induced YdiU will inactivate chaperones and promote their degradation. *Salmonella* might benefit from this process and survive under acute stress condition by turning off ATP consumption of chaperones effectively and rapidly in response to low ATP level. To verify the role of YdiU in energy management under stress condition, the intracellular levels of ATP in WT and ΔYdiU *Salmonella* during heat recovery were monitored. Notably, the intracellular concentration of ATP in ΔYdiU continuously decreased upon heat treatment, while that of wild-type *Salmonella* initially declined and then increased upon YdiU expression. Two hours post heat treatment, the ATP level of WT *Salmonella* has recovered to the level before heat, however, the one in ΔYdiU still remained in a very low level (Fig.10). Above data demonstrate the regulatory role of YdiU in energy utilization which might dramatically improve the survivability of *Salmonella* under acute heat stress.

UMPylation Occurs in Response to Stress in a YdiU-dependent Manner.

To further investigate the relationship between YdiU, UMPylation and heat stress signaling, experiments with WT and ΔYdiU *Salmonella* strain before or after heat treatment were performed (Supplementary Fig.S12). The level of YdiU and DnaK was measured by western blot. Agreeing with Fig.1d, YdiU is highly expressed in heat-treated WT *Salmonella* but not in the untreated one (Supplementary Fig.S12a). Subsequently, mass spectrometry-based proteomics were performed. Analyzed with ProteinPilot, twenty-three proteins with nucleotide-mediated PTMs (AMPylation, UMPylation and GMPylation) were identified in heat-treated WT *Salmonella* while only two of these modifications were identified in the untreated WT *Salmonella* suggesting nucleotide-mediated modifications might be induced in response to stress signaling (Supplementary Fig.S12b,c, Supplementary Table S5). No UMPylation of proteins were detected in ΔYdiU strain no matter with or without heat treatment suggesting UMPylation occurred in a YdiU-dependent manner (Supplementary Fig.S12b, d, Supplementary Table S5). Remarkably, proteins with AMP and GMP-modification were identified in heat-treated ΔYdiU

implying, in addition to YdiU, other unknown enzyme(s) might mediate the AMPylation and GMPylation of proteins in *Salmonella*.

DISCUSSION

The attachment of UMP to protein has been rarely reported. The sole identified prokaryotic UMPylator is the GlnD subunit from glutamine synthetase, acting to modify the GlnB subunit to modulate the synthesis rate of glutamine[22]. AvrAC, an effector from *Xanthomonas*, has been reported to UMPylate *Arabidopsis* BIK1 and RIPK, thereby inhibiting host immune signaling[33]. Intriguingly, AvrAC employs a Fic domain to achieve UMPylation activity, an unusual activity for this domain, as most other Fic domains modify targets with AMP[34, 35, 36]. YdiU shares no sequence identity with either GlnD or AvrAC, but UMPylates forty-six bacterial substrates. YdiU-dependent UMPylation occurs primarily on the tyrosine and histidine residues. To our knowledge, YdiU is the first known enzyme to catalyze the UMPylation of histidine. Histidine and tyrosine residues play significant roles in enzymatic catalysis and protein-protein interaction, so the linking of an UMP moiety to those residues may have a significant effect on protein function. Thus, we speculate that YdiU may act as a global regulator in bacteria through UMPylation process. These studies revealed an essential role of YdiU and UMPylation to regulate the function of the chaperone network and thermo-resistance of bacteria. Further study should explore these activities in higher eukaryotes.

Recently, Sreelatha *etal* reported the crystal structure of *P. syringae* YdiU-ATP and further identified YdiU as an AMPylator able to modify itself and two proteins involved in redox homeostasis[19]. Consistent with their finding, we found that YdiU exhibited *in vitro* self-AMPylation acitivity. However, mass spectrometric assays of YdiU-expressing *Salmonella* failed to detect AMPylation targets of YdiU, although this method was successfully used to detect dozens of targets with UMPylation. It is possible that the activity of YdiU to catalyze UMPylation or AMPylation depends on specific conditions to respond to different signals. Whether YdiU regulates cell activity through both AMPylation and UMPylation processes requires further investigation.

Before UMPylation identified in this study, phosphorylation and glutathionylation were reported to regulate the activities of bacterial chaperones. DnaK and GroEL can autophosphorylate themselves in response to high temperature, therefore acting to enhance their ATPase activity

and their affinity for unfolded proteins was enhanced[37, 38]. Glutathionylation of DnaK, however, acts reduce its activity by changing the secondary structure and tertiary conformation[39]. In higher eukaryotes, the activities of endoplasmic reticulum (ER)-localized Hsp70 chaperone BiP and cytosolic chaperone Ssa2 are regulated by AMPylation mediated by Fic domain proteins in response to unfolded protein stress or heat stress[40, 41, 42]. Recently, aggregation and toxicity of neurodegenerative disease-associated polypeptides was found to be modulated by the AMPylation of chaperone in elegan[43].

Nucleotide-mediated PTMs of chaperones were identified in prokaryote for the first time. Our data show that UMPylation of chaperones by YdiU inhibits their activities and promotes their degradation. The biological significance of YdiU-mediated UMPylation of chaperones might be related to the conservation of energy during stress condition. Recovery from stress is an energy-consuming process for bacteria, requiring few to thousands of ATPs to refold a single misfolded protein[44, 45]. Stresses frequently lead to the depletion of cellular ATP. When ATP is limited, turning off chaperones' activities by YdiU through UMPylation would allow bacteria to maintain sufficient energy for their basic life activities and protect bacteria form ATP depletion during recovery. The observation of the sharply decline of ATP in ΔYdiU strain during heat recovery but not in wild type *Salmonella* supports this hypothesis (Fig.10). Remarkably, our data showed YdiU could promote the degradation of chaperones. Under stress condition, bacteria need to estimate if they have the ability to repair the misfolded proteins, when it is helpless to handle with this situation by chaperones, it is better to switch form chaperone-mediated repairment to protease-mediated self-protection during acute stress and YdiU exactly functions in this process.

On the basis of above data, we propose a model in which YdiU modulates chaperone activity in response to both stress condition and ATP level (Fig.11). Firstly, the expression of YdiU is induced by stress. When the stress is mild or transient, only a fraction of proteins are damaged. Chaperones repair the misfolded proteins using a few ATP. At that time, YdiU is self-AMPylated and inactive. When the stress is acute and persistent, a mass of proteins denatured, the repairment mediated by chaperones consumes lots of ATP. Under ATP-limited condition, YdiU is activated as an UMPylator. Then, YdiU will UMPylate and inactive chaperones and promote the degradation of chaperones. It is possible that the degradation of other UMPylated substrates of YdiU is promoted as well. Then, bacteria switch from chaperone-mediated repairment to protease-mediated self-protection and keep sufficient energy for their survival.

MATERIAL AND METHODS

Bacterial strains and culture media

The bacterial strains used in this study are listed in Supplementary Table S6. For the experiments shown in Fig.1, *S. typhimurium* ATCC14028 culture was grown overnight and subcultured into corresponding medium. When the OD600 reached 0.4-0.5, bacterial cells were harvested for subsequent functional study. LB medium and M9 minimal medium were prepared as described previously[46]. H_2O_2-stress medium (H_2O_2) was LB medium supplemented with H_2O_2 to a final concentration of 1 mM. Iron-limited medium (Fe^-) was LB medium supplemented with 2,2-dipyridyl to a final concentration of 0.5 mM. Antibiotic -stress medium (AMP) was LB medium supplemented with 0.5 μg/mL Ampicillin. High osmotic stress medium were prepared by adding 300 mM NaCl (NaCl) or 20% w/v Glucose (Glu), respectively. Acid-stress medium (H^+) was LB medium supplemented with 0.5 μl/mL acetic acid (~pH 5.2). Envelop-stress medium (Indole) was LB medium adding indole to a final concentration of 2 mM. For the experiments shown in Fig. S1, YdiU was induced using LB medium supplemented with 0-0.2% L-arabinose.

For the experiments shown in Fig.1b and 9b, indicated strains were grown overnight in 10 mL LB medium. 50 μl above culture was subcultured into 5 mL LB medium. When the OD600 reached 0.4, strains were treated as indicated time at 50°C or 55°C. After recovery at 37°C for 30 min, bacterial cells were harvested for subsequent functional study.

RNA isolation and real-time quantitative PCR

Total RNA was isolated using the RNAprep Pure Bacteria Kit (TIANGEN). The reverse transcription reactions were performed using HiScript II Q-RT SuperMix (Nanjing Vazyme BioTech Co.,Ltd.) according to manufacturer's instructions and incubated at 42℃ for 60 min, followed by 10 min at 70℃. The quantitative RT-PCR reactions were performed on an Applied Biosystems 7500 Sequence Detection system (Applied Biosystems, Foster, CA, USA) using ChamQ SYBR Color qPCR Master Mix (Nanjing Vazyme BioTech Co.,Ltd.). GADPH was used as an internal reference.

Antibody preparation

Antibody against YdiU and GapA (reference) were prepared by Dia-An Biotech, Inc, in Wuhan, China. 2mg purified protein was mixed with FCA (Freund's complete adjuvant) or FIA (Freund's incomplete adjuvant), followed by injecting into two Japanese White rabbits four

times. FCA is only used in the first injection, while FIA for the rest injections. The 2nd injection is at 28th day since the first injection. And for other injections, 2 weeks intervals were needed between each injection. 3 days after the 4th injection, antiserum titer were tested by ELISA. The rabbits with higher titer was killed and bleeded at the 64th day since the first injection. The affinity column was made by coupling 1mg purified protein to CNBr-activated Sepharose 4B from GE. The antiserum was applied onto the column, the specific antibody were eluted with the Glycine HCl buffer at pH 2.5.

Western blot

Bacterial cells were lysed using 4×SDS-PAGE loading dye followed by heating at 95^{o}C for 10 min before SDS-PAGE. Total proteins on gels were transferred to nitrocellulose membranes at 250 mA for 2 h in transfer buffer (96 mM glycine, 12.5 mM Tris, and 10% methanol). The membranes were blocked in 5% milk in PBS-0.1% and Tween 20 (PBST) at 37^{o}C for 1h, followed by incubation with polyclonal antibody to YdiU (this study) diluted 1:2000, GapA (this study) diluted 1:5000, DnaK (Abcam) or GroEL (Novusbio) diluted 1:10000 in PBST overnight at 4^{o}C. The membranes were incubated with HRP-Conjugated Goat anti Rabbit or Mouse IgG (h+l) (Abcam) diluted 1:10000 in PBST at 37^{o}C for one hour after three washes with PBST. The membranes were then washed three times and then detected by chemiluminescence.

Construction of *ydiU* knock-out strain

S. *typhimurium* ATCC14028 strain was purchased from American Type Culture Collection. The *ydiU* gene knockout strain was constructed using the lambda Red recombinase system as described previously[47]. Briefly, the chloramphenicol resistance-FRT cassette was amplified from pKD3 by PCR with primers including the 5'and 3' flanking regions of the *ydiU* gene. The amplified product was transformed into *S. typhimurium* ATCC14028 strain containing the pKD46 plasmid, and then recombined colonies were selected on LB agar plates containing 25 μg/ml chloromycetin. PCR was then performed with another two primers to confirm the deletion of the *ydiU* gene. The pCP20 plasmid was then used to remove the chloramphenicol resistance gene. The *ydiU* knock-out strain of *E.coli* BL21 (DE3) was constructed as described above.

Plasmid construction

Plasmids used in this study are listed in Supplementary Table S6. For *in vivo* study described in the next section, *Salmonella* YdiU 1-475aa and *Salmonella* YdiU 1-475aa D256A was cloned

into the pBAD24 vector. For biochemical study, YdiU full-length protein,YdiU1-475aa, GroEL191-376aa, DnaK, HtpG 1-624aa, ClpB, GrpE, GrxA genes were amplified from *E.coli* str. K12 substr. MG1655 genomic DNA and cloned into an expression vector, pGL01, a modified vector based on pET15b with a PPase cleavage site to remove the His tag. Mutants of YdiU (Y71A, K107A, D119A, E130A, N244A, D246A, N247A, D256A, T112A, S115A, R116A, F76A, V242A, Y281A), GroEL191-376aa (Y199F, Y203F, Y199F-Y203F, Y199F-Y203F-Y360F) were constructed using a two-step PCR strategy and separately cloned into pGL01.

Sample preparation for mass spectrometry

The recombinant plasmid encoding *Salmonella* YdiU1-475aa was transformed into the *ydiU* knockout strain to generate the YdiU-expressed strain (pYdiU) while empty pBAD24 was transformed into the *ydiU* knockout mutant as a negative control (ΔYdiU). Both ΔYdiU and pYdiU strains were grown overnight in LB medium with 100 μg/ml Ampicillin to select for the plasmids, and then subcultured into 10 mL LB medium with 100 μg/ml Ampicillin. When the OD600 reached 0.4-0.6, 0.1% L-arabinose was added to induce YdiU expression. Bacterial cells were harvested 4 hours later and lysed using a buffer containing 4 % SDS, 100mM Tris-HCl pH7.6, 1mM DTT and lysozyme. After centrifugation at 14000 rpm for 40 min, the supernatant was removed and quantified with the BCA Protein Assay Kit (Bio-Rad, USA). Samples containing 200 μg of proteins were purified by ultrafiltration, incubated with iodoacetamide to block reduced cysteine residues, and then digested with 4 μg trypsin at 37 ^{o}C overnight. Peptides of each sample were desalted on C18 Cartridges and concentrated by vacuum centrifugation and reconstituted in 40 μl of 0.1% (v/v) formic acid.

Mass spectrometry

Peptides were fractionated by SCX chromatography using the AKTA Purifier system (GE Healthcare) and injected for nanoLC-MS/MS analysis. LC-MS/MS analysis was performed on a Q Exactive mass spectrometer (Thermo Scientific) that was coupled to Easy nLC (Proxeon Biosystems, now Thermo Fisher Scientific) for 240 min in positive ion mode. MS/MS spectra were automatically searched against the Uniprot_Salmonella_typhimurium_99287 database using the ProteinPilot software 4.5 (AB Sciex) to identify the protein fragments and the protein identification results were obtained. UMPylated peptides, AMPylated peptides and GMPylated peptides were identified by searching for the modification 'PhosphoUridine', 'Phosphoadenosine', 'Phosphoguanosine', respectively.

Protein expression and purification

Proteins were expressed in *E. coli* BL21(DE3). When the OD600 reached 0.4-0.6, cultures were cooled to 16ºC and induced overnight by 0.01-0.1 mM IPTG. Harvested cells were lysed by sonication. Proteins were purified by Ni^{2+}-NTA affinity column. The His-tag of the proteins was removed by PPase treatment[48]. Then proteins were then concentrated and purified by Superdex 200 chromatography. Selenomethionine-labeled YdiU was expressed in *E. coli* BL21(DE3) using the methionine biosynthesis inhibition method[49].

Crystallization and structure determination

$YdiU^{475}$ was concentrated to 10 mg/ml. Crystals of Apo-YdiU were grown by hanging drop vapour diffusion in a buffer containing 10% PEG200; 0.1M Bis-Tris propane pH9.0; 18% PEG8,000. To obtain YdiU-AMPPNP, 10mM AMPPNP and $MgCl_2$ were added to YdiU and crystals of YdiU-AMPPNP appeared in a buffer containing 2.8 M Sodium acetate pH7.0 and 0.1 M Bis-Tris propane pH7.0. Diffraction data of the above crystals were collected at the Shanghai Synchrotron Radiation facility (SSRF) using beamlines BL17u1 and BL19ul. The data sets were processed using the HKL2000 software suite[50]. The structure of YdiU-AMPPNP was solved by selenium single wavelength anomalous diffraction and those of YdiU-AMP-PPi and of Apo-YdiU were solved by molecular replacement. The initial model was generated using the program Autosolve[51]. The subsequent model was manually built using COOT and refined using PHENIX[32, 52]. The data collection and structure refinement statistics are summarized in Supplementary Table S7. Structural figures were generated using PyMol (http://www.pymol.org).

Molecular docking

UTP was docked to the binding site of YdiU using Autodock Tools 1.5.6 performing with flexible UTP molecule and the rigid YdiU[53]. Moreover, Amber ff14SB force field were used to obtain the appropriate conformations and binding positions of UTP by energy optimization[54]. Finally, the structure with the lowest docking energy was used as the final model for YdiU-UTP. The number of grid points in the XYZ of grid box was set to 40×40×40, the grid spacing was 0.375 Å, the number of GA run was set to 100, the rest parameters were set to default. Finally, the structure with the lowest docking energy was carried out with energy minimization. The optimization process is carried out in two steps: firstly, the steepest descent method optimization of 2000 steps, then, the structure was further optimized by the 2000 steps with conjugate gradient method.

Molecular dynamics simulation

MD simulation of YdiU-ATP or YdiU-UTP complex was applied using Amber 18 software package, respectively[55]. Amber ff14SB force field was applied, in which the coordination of Mg^{2+} with the surrounding residues was optimized by MCPB[56]. The parameters of protein field are based on experimental condition. The simulated temperature set as 300 K and the pH as 7.0. The solutes were solvated in a truncated periodic box with a 1.0 nm distance solute-wall using the TIP3P water model[57]. Prior to MD simulation, the system was optimized by two steps: First, the solute was constrained, and the water solvent was optimized using 5000 steps with steepest descent method and 5000 steps with conjugate gradient method. Second, unrestrained minimizations of the whole systems were executed with another 5000 steps of steepest descent and 5000 steps of conjugate gradient. The MD simulation process was also carried out in two stages: First, the 100ps constrained solute MD simulation was performed in which system temperature was gradually raised from 0K to 300K; Then 50 ns unconstrained constant temperature MD simulation was performed. In the simulation process, the SHAKE algorithm was applied to constrain covalent bonds including hydrogen atoms[58]. The MD time step was set as 2 fs, and one snapshot was taken every 10 ps (1 ps), thus 5,000 conformations were obtained in each MD simulation. The MD simulation dynamic process was monitored with the VMD software package[59]. The binding free energy (ΔG_{bind}) was calculated as described before[60].

***In vitro* UMPylation assay with α^{32}P-UTP**

For the data shown in Fig.3d, 2 μg of purified $YdiU^{475}$ or $YdiU^{fl}$ was incubated in an UMPylation reaction buffer containing 25 mM Tris-HCl (pH7.5), 1 mM DTT, 25 mM $MgCl_2$/$CaCl_2$/$ZnCl_2$/$MnCl_2$, and 2 μCi α^{32}P-UTP at 30 °C for 30 min. Then products were analyzed using 12% NuPAGE gels and imaged by autoradiograph.

For the experiment shown in Fig.3e, 8 μg of the corresponding chaperones was incubated with or without 1 μg $YdiU^{475}$ in the reaction buffer with 25 mM $MnCl_2$ and 2 μCi α^{32}P-UTP at 30 °C for 30 min, then analyzed using 12% NuPAGE gel and imaged by autoradiograph.

***In vitro* UMPylation assay with Biotin-16-UTP**

For the experiment shown in Fig.3f, 8 μg of purified chaperones were incubated with or without 1 μg $YdiU^{475}$ in the buffer containing 25 mM Tris-HCl (pH8.5), 1 mM DTT, 100 mM NaCl, 10 mM $MnCl_2$, and 500 μM Biotin-16-UTP. For the experiment shown in Fig.4a-b, 2 μg of $YdiU^{475}$ was incubated in the buffer containing 25 mM Tris-HCl (pH7.5), 1 mM DTT, 100 mM NaCl, 10

mM $MnCl_2$, 10 mM $MgCl_2$ and Biotin-16-UTP or Biotin-17-ATP in increasing concentration (0 μM, 0.1 μM, 0.3 μM, 1 μM, 3 μM, 10 μM, 30 μM, and 100 μM). For the experiment shown in Fig.4c, 1 μg $YdiU^{FL}$ or $YdiU^{475}$ were used to modify 2 μg GroEL in a buffer containing 25 mM Tris-HCl (pH7.5), 1 mM DTT, 100 mM NaCl, 10 mM $MnCl_2$, 10 mM $MgCl_2$ and 100 μM Biotin-16-UTP or Biotin-17-ATP. For the experiment shown in Fig.6j, Fig.S7c, and Fig.8b, 1 μg native YdiU or variants was incubated with 2 μg native GroEL or variants in the same buffer as the experiment in Fig.3f. After incubation at 30 °C for 1h, the above reaction products were resolved by 12% NuPAGE gel and transferred to nitrocellulose membranes. The membranes were stained in 0.1% Ponceau S with shaking for 5 min at room temperature, and then washed three times with ddH_2O. The Streptavidin HRP blot was performed as previously described[61]. Briefly, the membranes were incubated in BSA blocking buffer (1×PBS containing 1% BSA and 0.2% Triton X-100) with shaking for 30 min at room temperature. Next, the membranes were incubated with streptavidin-HRP at 1:40,000 dilution in BSA blocking buffer overnight at 4°C. The membranes were washed three times with 1×PBS and then blocked with ABS blocking buffer (1×PBS containing 10% adult bovine serum and 1% Triton X-100) with shaking for 5 min at room temperature. Membranes were washed three times with 1×PBS and blots were developed and visualized using a enhanced chemiluminescence (ECL) kit.

For the experiment shown in Fig.5, AMPylated $YdiU^{fl}$ and $YdiU^{475}$ were product in a reaction buffer containing 25 mM Tris-HCl (pH7.5), 1 mM DTT, 10 mM $MgCl_2$ and 10 mM ATP at 30°C for 4 h and purified using desalting column (GE, PD MiniTrap G-25) to remove ATP and Mg^{2+}. Then 1 μg AMPylated or non-AMPylated YdiU was incubated with 2 μg purified GroEL in the UMPylation buffer containing 25 mM Tris-HCl (pH7.5), 1 mM DTT, 10 mM $MnCl_2$ and 100 μM Biotin-16-UTP at 30°C for 10min or 60 min.

Biolayer interferometry (BLI) assay

Biolayer interferometry experiments were performed using an Octet RED96 instrument (ForteBio) at 25°C. To study the interaction between YdiU and UTP or ATP analog (Fig.4d-e), purified $YdiU^{475}$ was incubated with EZ-Link-Biotin (MCR=3:1) at 25°C for 30 min, and then purified with desalting column (GE, PD MiniTrap G-25). About 100 μg/ml YdiU was loading onto each Super Streptavidin senor (ForteBio, 18-5057) in PBS buffer. Following a baseline step the sensors were introduced to 0-200 μM UMPNPP or AMPNPP for 60s to measure the association response, and then changed to PBS buffer for 60s to measure dissociation. Data were

processed by double deduction with a sensor control and buffer control. To study the effect of UMPylation on the interaction between DnaK and GrpE (Fig.8e), experiments were performed as described in Fig.S11. Briefly, DnaK proteins were biotinylated either by EZ-Link-Biotin or by biotin-16-UTP and YdiU, and then separately loaded to Streptavidin sensors. The sensors were introduced to PBS containing 10 μg/ml GrpE to measure the association response and changed to PBS buffer to measure dissociation. Data were processed by deduction with sensor control.

Isothermal titration calorimetry (ITC) assay

The ITC experiments were executed at 25°C using an iTC200 microcalorimeter (Malvern). All samples were prepared in a buffer containing 20 mM Tris HCl (pH 8.0) and 100 mM NaCl, and then 1.5 mM UMPNPP or AMPNPP was injected into the calorimetric cell containing 0.1 mM YdiU. ITC data were analyzed using MicroCal Origin 7.0 software.

Streptavidin pull-down assay

The streptavidin pull-down assay (SA pull-down) was performed as described in Fig.S9. Briefly, native GroEL and the GroEL Y199F,Y203F mutant were separately biotinylated by EZ-Link-Biotin and purified by desalting column. Next, 50 μg native GroEL was incubated with 20 μg $YdiU^{475}$ (with His-tag) and 500 μM Biotin-16-UTP in a reaction buffer containing 25 mM Tris-HCl (pH7.5), 100 mM NaCl,1 mM DTT, 10 mM $MnCl_2$ at 30°C for 2 h and purified by NTA Ni column and desalting column to remove free YdiU and Biotin-16-UTP. Next, 20 μg of the proteins were loaded to 50 μl High Capacity Streptavidin Agarose and washed three times with wash buffer containing 25 mM Tris-HCl (pH 8.0) and 100 mM NaCl[62]. Separately, 50 μg human ornithine carbamoyltransferase (OTC) was denatured by 8 M Urea. The denatured OTC proteins were then diluted by a factor of 50 into wash buffer and immediately added to the resin with GroEL protein and then incubated at 37 °C for 30 min. After washing twice with wash buffer, the proteins were eluted by 8 M Urea (pH 1.5) and resolved by 12% NuPAGE gel.

***In vitro* degradation assay of chaperones**

The expression plasmids of GroEL191-376aa and DnaK were tranformed into *ydiU* knock-out strain of *E.coli* BL21 (DE3). The processes of bacteria culture and protein expression were performed as described above. After sonication, $YdiU^{475aa}$or $YdiU^{475aa}$ D256A was added into the samples at a final concentration of 5mg/ml and incubated at 30 °C for the indicated time. Then the total proteins were analyzed using 12.5% SDS-PAGE gel.

Thermal resistance of wild type and ΔYdiU *Salmonella*

The survival rates of the *S. typhimurium* ATCC14028 wild type strain and the ΔYdiU strain after heat treatment were determined[63, 64]. First, overnight cultures of WT and ΔYdiU were transferred into 10 ml of fresh LB medium, and when the culture OD reached 0.5, cells were harvested by centrifugation. The cell pellets were washed twice and resuspended in 0.9% NaCl solution. The samples were then divided, with some aliquots treated at 55 °C for corresponding times and the remainder serving as controls without heat treatment. Cells were plated as a dilution series on LB plates and cultured overnight at 37 °C. The next day, the viable counts of bacteria were detected as the number of colony forming units. All experiments were performed with four repeats and the results presented are mean values.

Measurement of intracellular ATP levels

Overnight cultures of WT and ΔYdiU *Salmonella* were transferred into 20 ml of M9 minimal medium supplemented with 0.4% glucose, and when the culture OD reached 0.6, cells were treated at 55 °C for 1 min. Then, the cultures were divided into eight samples, which were allowed to recover at 37 °C for 5 min, 10 min, 20 min, 30 min, 45min, 60 min, 90 min, or 120 min respectively. After incubation, the OD value of each culture was detected. The cells of each sample were harvested by centrifugation at 12000 rpm for 2 min at 4°C and lysed by lysozyme. Then the ATP levels of these samples were measured by the luciferin-luciferase method[65] following the protocol of an ATP detection kit (Beyotime, China). The average amount of intracellular ATP was obtained by calculating the ratio of total ATP and OD_{600}.

DATA AVAILABILITY

The X-ray structures (coordinates and structure factor files) of YdiU have been submitted to PDB under accession number 6INY (YdiU-AMPPNP), 6III (YdiU-AMP-imidodiphosphonic acid) and 6K20 (Apo-YdiU).

Mass spectrometry based data were submitted to ProteomeXchange under accession number PXD013825.

ACKNOWLEDGEMENT

We thank the staff at beamline BL17Ul and BL19Ul at the Shanghai Synchrotron Radiation facility for supporting data collection of protein crystals.

Author contributions: B.L. and L.G. designed the study; YL.Y., YY.Y., Y.M. and H.D. purified proteins; YL.Y., YY.Y., C.L. and H.L. performed *in vitro* experiments; F.Z. constructed *ydiU* knock-out strain; N.S., Y.W., P.L. and X.L. performed *in vivo* experiments; B.L., Z.Y. and L.G. performed structural experiments; YL.Y., W.W. and H.J. performed BLI assay; B.L., YY.Y., C.L. and YL.Y. analyzed data; B.L. wrote the manuscript.

FUNDING

This work was supported by National Natural Science Foundation of China [31500050, 31800054 and 31270786]. The Innovation Project of Shandong Academy of Medical Sciences. the Natural Science Foundation of Shandong Province [ZR2017MH020]. The Department of Health and Family-plan Bureau, Shandong Province [2016WS0525].

Conflict of interest statement. None declared.

REFERENCES

1. Browning DF, Busby SJ. The regulation of bacterial transcription initiation. *Nature reviews Microbiology* 2004, **2**(1)**:** 57-65.

2. Helmann JD, Chamberlin MJ. Structure and function of bacterial sigma factors. *Annual review of biochemistry* 1988, **57:** 839-872.

3. Balleza E, Lopez-Bojorquez LN, Martinez-Antonio A, Resendis-Antonio O, Lozada-Chavez I, Balderas-Martinez YI*, et al.* Regulation by transcription factors in bacteria: beyond description. *FEMS microbiology reviews* 2009, **33**(1)**:** 133-151.

4. Hoch JA. Two-component and phosphorelay signal transduction. *Current opinion in microbiology* 2000, **3**(2)**:** 165-170.

5. Stock AM, Robinson VL, Goudreau PN. Two-component signal transduction. *Annual review of biochemistry* 2000, **69:** 183-215.

6. Hu LI, Lima BP, Wolfe AJ. Bacterial protein acetylation: the dawning of a new age. *Molecular microbiology* 2010, **77**(1)**:** 15-21.

7. Jones JD, O'Connor CD. Protein acetylation in prokaryotes. *Proteomics* 2011, **11**(15)**:** 3012-3022.

8. Carabetta VJ, Cristea IM. Regulation, Function, and Detection of Protein Acetylation in Bacteria. *Journal of bacteriology* 2017, **199**(16).

9. Dukan S, Nystrom T. Bacterial senescence: stasis results in increased and differential oxidation of cytoplasmic proteins leading to developmental induction of the heat shock

regulon. *Genes & development* 1998, **12**(21)**:** 3431-3441.

10. Schwarz F, Aebi M. Mechanisms and principles of N-linked protein glycosylation. *Current opinion in structural biology* 2011, **21**(5)**:** 576-582.

11. Cain JA, Solis N, Cordwell SJ. Beyond gene expression: the impact of protein post-translational modifications in bacteria. *Journal of proteomics* 2014, **97:** 265-286.

12. Grangeasse C, Stulke J, Mijakovic I. Regulatory potential of post-translational modifications in bacteria. *Frontiers in microbiology* 2015, **6:** 500.

13. Dudkiewicz M, Szczepinska T, Grynberg M, Pawlowski K. A novel protein kinase-like domain in a selenoprotein, widespread in the tree of life. *PLoS One* 2012, **7**(2)**:** e32138.

14. Galperin MY, Koonin EV. 'Conserved hypothetical' proteins: prioritization of targets for experimental study. *Nucleic acids research* 2004, **32**(18)**:** 5452-5463.

15. Galperin MY, Koonin EV. From complete genome sequence to 'complete' understanding? *Trends Biotechnol* 2010, **28**(8)**:** 398-406.

16. Erasmus DJ, van der Merwe GK, van Vuuren HJ. Genome-wide expression analyses: Metabolic adaptation of Saccharomyces cerevisiae to high sugar stress. *FEMS yeast research* 2003, **3**(4)**:** 375-399.

17. Phadtare S, Inouye M. Genome-wide transcriptional analysis of the cold shock response in wild-type and cold-sensitive, quadruple-csp-deletion strains of Escherichia coli. *Journal of bacteriology* 2004, **186**(20)**:** 7007-7014.

18. Hsu-Ming W, Naito K, Kinoshita Y, Kobayashi H, Honjoh K, Tashiro K*, et al.* Changes in transcription during recovery from heat injury in Salmonella typhimurium and effects of BCAA on recovery. *Amino acids* 2012, **42**(6)**:** 2059-2066.

19. Sreelatha A, Yee SS, Lopez VA, Park BC, Kinch LN, Pilch S*, et al.* Protein AMPylation by an Evolutionarily Conserved Pseudokinase. *Cell* 2018, **175**(3)**:** 809-821 e819.

20. Gragerov A, Nudler E, Komissarova N, Gaitanaris GA, Gottesman ME, Nikiforov V. Cooperation of GroEL/GroES and DnaK/DnaJ heat shock proteins in preventing protein misfolding in Escherichia coli. *Proceedings of the National Academy of Sciences of the United States of America* 1992, **89**(21)**:** 10341-10344.

21. Thomas JG, Baneyx F. ClpB and HtpG facilitate de novo protein folding in stressed Escherichia coli cells. *Molecular microbiology* 2000, **36**(6)**:** 1360-1370.

22. Adler SP, Purich D, Stadtman ER. Cascade control of Escherichia coli glutamine synthetase. Properties of the PII regulatory protein and the uridylyltransferase-uridylyl-removing enzyme. *The Journal of biological chemistry* 1975, **250**(16)**:** 6264-6272.

23. Kehres DG, Zaharik ML, Finlay BB, Maguire ME. The NRAMP proteins of Salmonella typhimurium and Escherichia coli are selective manganese transporters involved in the response to reactive oxygen. *Molecular microbiology* 2000, **36**(5)**:** 1085-1100.

24. Jakubovics NS, Jenkinson HF. Out of the iron age: new insights into the critical role of manganese homeostasis in bacteria. *Microbiology* 2001, **147**(Pt 7)**:** 1709-1718.

25. Liu C, Heath LS, Turnbough CL, Jr. Regulation of pyrBI operon expression in Escherichia coli by UTP-sensitive reiterative RNA synthesis during transcriptional initiation. *Genes & development* 1994, **8**(23)**:** 2904-2912.

26. Fenton WA, Kashi Y, Furtak K, Horwich AL. Residues in chaperonin GroEL required for polypeptide binding and release. *Nature* 1994, **371**(6498)**:** 614-619.

27. Buckle AM, Zahn R, Fersht AR. A structural model for GroEL-polypeptide recognition. *Proceedings of the National Academy of Sciences of the United States of America* 1997, **94**(8)**:** 3571-3575.

28. Shiau AK, Harris SF, Southworth DR, Agard DA. Structural Analysis of E. coli hsp90 reveals dramatic nucleotide-dependent conformational rearrangements. *Cell* 2006, **127**(2)**:** 329-340.

29. Liberek K, Marszalek J, Ang D, Georgopoulos C, Zylicz M. Escherichia coli DnaJ and GrpE heat shock proteins jointly stimulate ATPase activity of DnaK. *Proceedings of the National Academy of Sciences of the United States of America* 1991, **88**(7)**:** 2874-2878.

30. Harrison CJ, Hayer-Hartl M, Di Liberto M, Hartl F, Kuriyan J. Crystal structure of the nucleotide exchange factor GrpE bound to the ATPase domain of the molecular chaperone DnaK. *Science* 1997, **276**(5311)**:** 431-435.

31. Lee S, Sowa ME, Watanabe YH, Sigler PB, Chiu W, Yoshida M*, et al.* The structure of ClpB: a molecular chaperone that rescues proteins from an aggregated state. *Cell* 2003, **115**(2)**:** 229-240.

32. Emsley P, Cowtan K. Coot: model-building tools for molecular graphics. *Acta Crystallogr D Biol Crystallogr* 2004, **60**(Pt 12 Pt 1)**:** 2126-2132.

33. Feng F, Yang F, Rong W, Wu X, Zhang J, Chen S*, et al.* A Xanthomonas uridine 5'-monophosphate transferase inhibits plant immune kinases. *Nature* 2012, **485**(7396)**:** 114-118.

34. Worby CA, Mattoo S, Kruger RP, Corbeil LB, Koller A, Mendez JC*, et al.* The fic domain: regulation of cell signaling by adenylylation. *Mol Cell* 2009, **34**(1)**:** 93-103.

35. Yarbrough ML, Li Y, Kinch LN, Grishin NV, Ball HL, Orth K. AMPylation of Rho

GTPases by Vibrio VopS disrupts effector binding and downstream signaling. *Science* 2009, **323**(5911)**:** 269-272.

36. Casey AK, Orth K. Enzymes Involved in AMPylation and deAMPylation. *Chem Rev* 2018, **118**(3)**:** 1199-1215.

37. McCarty JS, Walker GC. DnaK as a thermometer: threonine-199 is site of autophosphorylation and is critical for ATPase activity. *Proceedings of the National Academy of Sciences of the United States of America* 1991, **88**(21)**:** 9513-9517.

38. Sherman M, Goldberg AL. Heat shock-induced phosphorylation of GroEL alters its binding and dissociation from unfolded proteins. *The Journal of biological chemistry* 1994, **269**(50)**:** 31479-31483.

39. Zhang H, Yang J, Wu S, Gong W, Chen C, Perrett S. Glutathionylation of the Bacterial Hsp70 Chaperone DnaK Provides a Link between Oxidative Stress and the Heat Shock Response. *The Journal of biological chemistry* 2016, **291**(13)**:** 6967-6981.

40. Ham H, Woolery AR, Tracy C, Stenesen D, Kramer H, Orth K. Unfolded protein response-regulated Drosophila Fic (dFic) protein reversibly AMPylates BiP chaperone during endoplasmic reticulum homeostasis. *The Journal of biological chemistry* 2014, **289**(52)**:** 36059-36069.

41. Sanyal A, Chen AJ, Nakayasu ES, Lazar CS, Zbornik EA, Worby CA*, et al.* A novel link between Fic (filamentation induced by cAMP)-mediated adenylylation/AMPylation and the unfolded protein response. *The Journal of biological chemistry* 2015, **290**(13)**:** 8482-8499.

42. Truttmann MC, Zheng X, Hanke L, Damon JR, Grootveld M, Krakowiak J*, et al.* Unrestrained AMPylation targets cytosolic chaperones and activates the heat shock response. *Proceedings of the National Academy of Sciences of the United States of America* 2017, **114**(2)**:** E152-E160.

43. Truttmann MC, Pincus D, Ploegh HL. Chaperone AMPylation modulates aggregation and toxicity of neurodegenerative disease-associated polypeptides. *Proceedings of the National Academy of Sciences of the United States of America* 2018, **115**(22)**:** E5008-E5017.

44. Diamant S, Goloubinoff P. Temperature-controlled activity of DnaK-DnaJ-GrpE chaperones: protein-folding arrest and recovery during and after heat shock depends on the substrate protein and the GrpE concentration. *Biochemistry* 1998, **37**(27)**:** 9688-9694.

45. Sharma SK, De los Rios P, Christen P, Lustig A, Goloubinoff P. The kinetic parameters and energy cost of the Hsp70 chaperone as a polypeptide unfoldase. *Nature chemical biology* 2010, **6**(12)**:** 914-920.

46. Wada T, Morizane T, Abo T, Tominaga A, Inoue-Tanaka K, Kutsukake K. EAL domain protein YdiV acts as an anti-FlhD4C2 factor responsible for nutritional control of the flagellar regulon in Salmonella enterica Serovar Typhimurium. *Journal of bacteriology* 2011, **193**(7)**:** 1600-1611.

47. Datsenko KA, Wanner BL. One-step inactivation of chromosomal genes in Escherichia coli K-12 using PCR products. *Proceedings of the National Academy of Sciences of the United States of America* 2000, **97**(12)**:** 6640-6645.

48. Li B, Yue Y, Yuan Z, Zhang F, Li P, Song N*, et al.* Salmonella STM1697 coordinates flagella biogenesis and virulence by restricting flagellar master protein FlhD4C2 from recruiting RNA polymerase. *Nucleic acids research* 2017, **45**(17)**:** 9976-9989.

49. Hendrickson WA, Horton JR, LeMaster DM. Selenomethionyl proteins produced for analysis by multiwavelength anomalous diffraction (MAD): a vehicle for direct determination of three-dimensional structure. *EMBO J* 1990, **9**(5)**:** 1665-1672.

50. Otwinowski Z, Minor W. Processing of X-ray diffraction data collected in oscillation mode. *Methods Enzymol* 1997, **276:** 307-326.

51. Terwilliger TC. Automated structure solution, density modification and model building. *Acta Crystallogr D Biol Crystallogr* 2002, **58**(Pt 11)**:** 1937-1940.

52. Adams PD, Grosse-Kunstleve RW, Hung LW, Ioerger TR, McCoy AJ, Moriarty NW*, et al.* PHENIX: building new software for automated crystallographic structure determination. *Acta Crystallogr D Biol Crystallogr* 2002, **58**(Pt 11)**:** 1948-1954.

53. Goodsell DS, Morris GM, Olson AJ. Automated docking of flexible ligands: applications of AutoDock. *Journal of molecular recognition : JMR* 1996, **9**(1)**:** 1-5.

54. Maier JA, Martinez C, Kasavajhala K, Wickstrom L, Hauser KE, Simmerling C. ff14SB: Improving the Accuracy of Protein Side Chain and Backbone Parameters from ff99SB. *Journal of chemical theory and computation* 2015, **11**(8)**:** 3696-3713.

55. Case DA, Cheatham TE, 3rd, Darden T, Gohlke H, Luo R, Merz KM, Jr.*, et al.* The Amber biomolecular simulation programs. *Journal of computational chemistry* 2005, **26**(16)**:** 1668-1688.

56. Li P, Merz KM, Jr. MCPB.py: A Python Based Metal Center Parameter Builder. *Journal of chemical information and modeling* 2016, **56**(4)**:** 599-604.

57. Price DJ, Brooks CL, 3rd. A modified TIP3P water potential for simulation with Ewald summation. *The Journal of chemical physics* 2004, **121**(20)**:** 10096-10103.

58. Coleman TG, Mesick HC, Darby RL. Numerical integration: a method for improving solution stability in models of the circulation. *Annals of biomedical engineering* 1977,

5(4)**:** 322-328.

59. Humphrey W, Dalke A, Schulten K. VMD: visual molecular dynamics. *Journal of molecular graphics* 1996, **14**(1)**:** 33-38, 27-38.

60. Woo HJ, Roux B. Calculation of absolute protein-ligand binding free energy from computer simulations. *Proceedings of the National Academy of Sciences of the United States of America* 2005, **102**(19)**:** 6825-6830.

61. Roux KJ, Kim DI, Burke B. BioID: a screen for protein-protein interactions. *Curr Protoc Protein Sci* 2013, **74:** Unit 19 23.

62. Rybak JN, Scheurer SB, Neri D, Elia G. Purification of biotinylated proteins on streptavidin resin: a protocol for quantitative elution. *Proteomics* 2004, **4**(8)**:** 2296-2299.

63. Jenkins DE, Schultz JE, Matin A. Starvation-induced cross protection against heat or H2O2 challenge in Escherichia coli. *Journal of bacteriology* 1988, **170**(9)**:** 3910-3914.

64. Blackburn CW, Curtis LM, Humpheson L, Billon C, McClure PJ. Development of thermal inactivation models for Salmonella enteritidis and Escherichia coli O157:H7 with temperature, pH and NaCl as controlling factors. *International journal of food microbiology* 1997, **38**(1)**:** 31-44.

65. St John JB. Determination of ATP in Chlorella with the luciferin-luciferase enzyme system. *Analytical biochemistry* 1970, **37**(2)**:** 409-416.

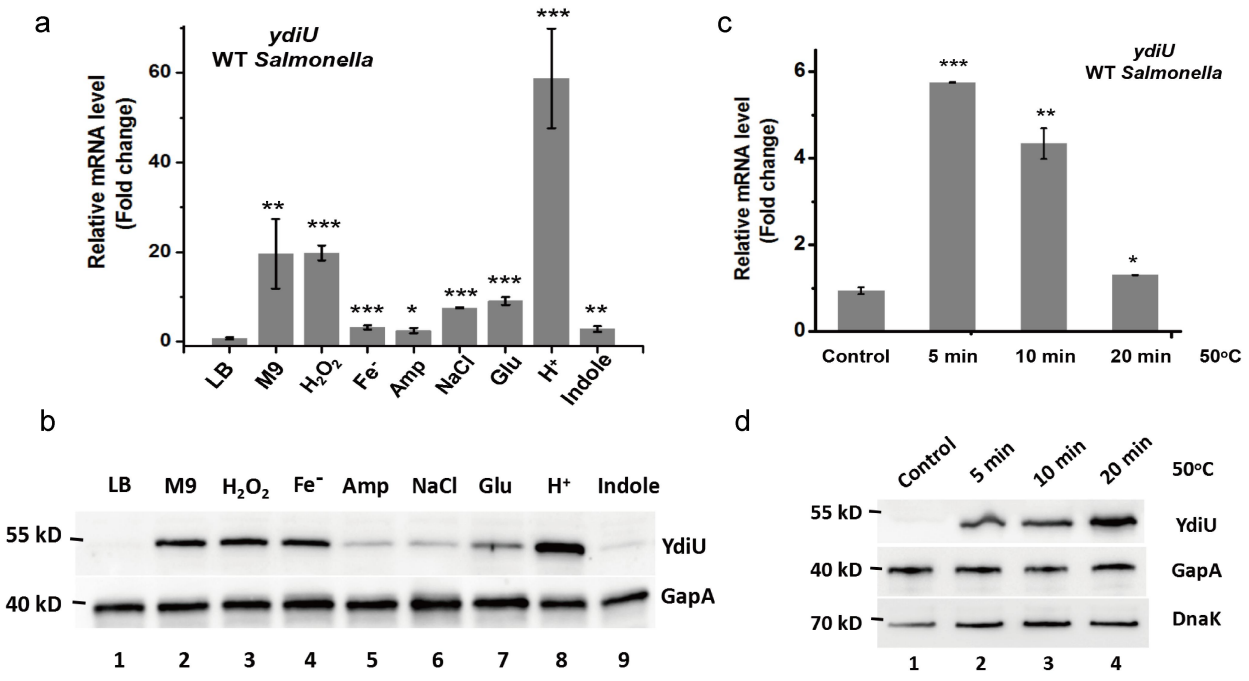

Fig.1. The expression of YdiU is stress-dependent in *Salmonella*.

(**a**) *Salmonella* were cultivated under different conditions, and the intracellular concentration of ydiU mRNA was detected by qRT-PCR. The statistical significance is indicated by ***P < 0.001, **P < 0.005, *P < 0.01, as compared to the concentration in LB medium using a t-test. (**b**) *Salmonella* were cultivated under different conditions, and the expression of YdiU was quantified by western blot. GapA (also known as GADPH) was used as a loading control. (**c**) The intracellular concentration of ydiU mRNA during 30 min recovery from 5-20 min heat treatment at 50°C. Statistical significance is indicated by ***P < 0.001, **P < 0.005 and *P < 0.01, as compared with the concentration without heat treatment. (**d**) The expression levels of YdiU and DnaK during recovery from heat injury. GapA was used as a loading control. Lane 1 is the negative control without heat treatment.

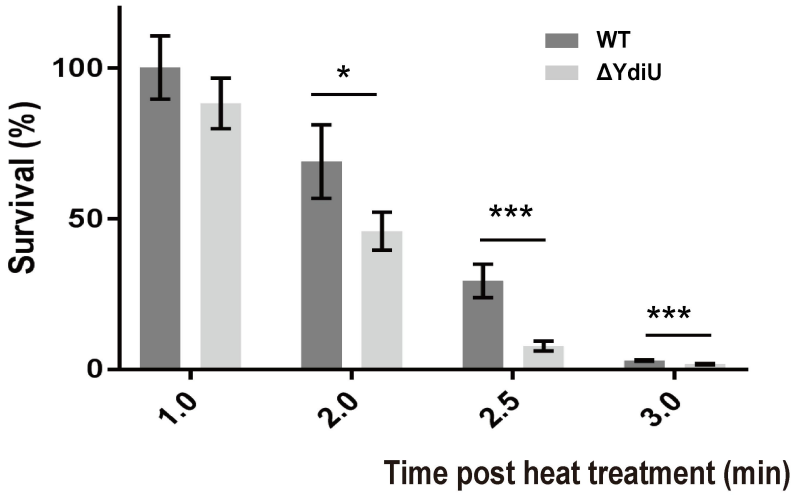

Fig.2. YdiU protects *Salmonella* form acute heat injury.

Survival ratios of WT and ΔYdiU *Salmonella* were detected following treatment at 55°C for 1min, 2min, 2.5 min, and 3 min. All experiments were performed as four replicates and the mean values are presented. Statistical significance is indicated by *P < 0.05 and ***P < 0.001 using a t-test.

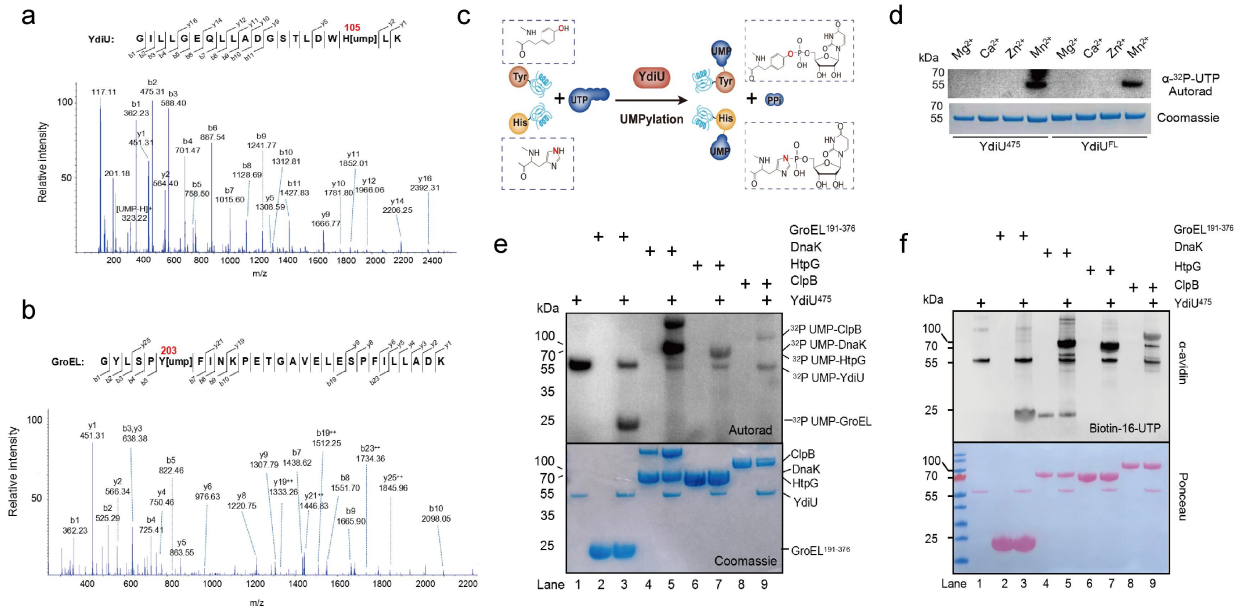

Fig.3. YdiU mediated self-UMPylation and UMPylation of chaperones.

(**a-b**) Electrospray ionization MS/MS spectra of UMP-modified peptides identified *in vivo*. The b and y ions are marked and indicated along the peptide sequence above the spectra. (**a**) YdiU peptide with an UMP-modified Histidine. An increased mass of 306.025 daltons was detected after y5, indicating that His105 was the UMP-modified residue. (**b**) GroEL peptide with an UMP-modified Tyrosine. The increased mass of 306.025 daltons started with b7. (**c**) Diagram for YdiU-mediated UMPylation. (**d**) Self-UMPylation of YdiU performed with different metal ions. YdiU^{fl} and YdiU^{475} were incubated with α^{32}P-UTP and corresponding divalent ions, followed by SDS-PAGE and autoradiography. (**e**) *In vitro* UMPylation of chaperones mediated by YdiU using α^{32}P-UTP as donor. UMPylation assays were performed with YdiU^{475} and the indicated recombinant candidate substrates in a reaction buffer containing α^{32}P-UTP and $MnCl_2$. (**f**) *In vitro* UMPylation of chaperones mediated by YdiU using biotin-16-UTP as donor. UMPylation assays were performed with YdiU^{475} and the indicated recombinant candidate substrates performed with biotin-16-UTP and $MnCl_2$ followed by avidin blotting. Total proteins were visualized by Ponceau S staining of the blot before blocking.

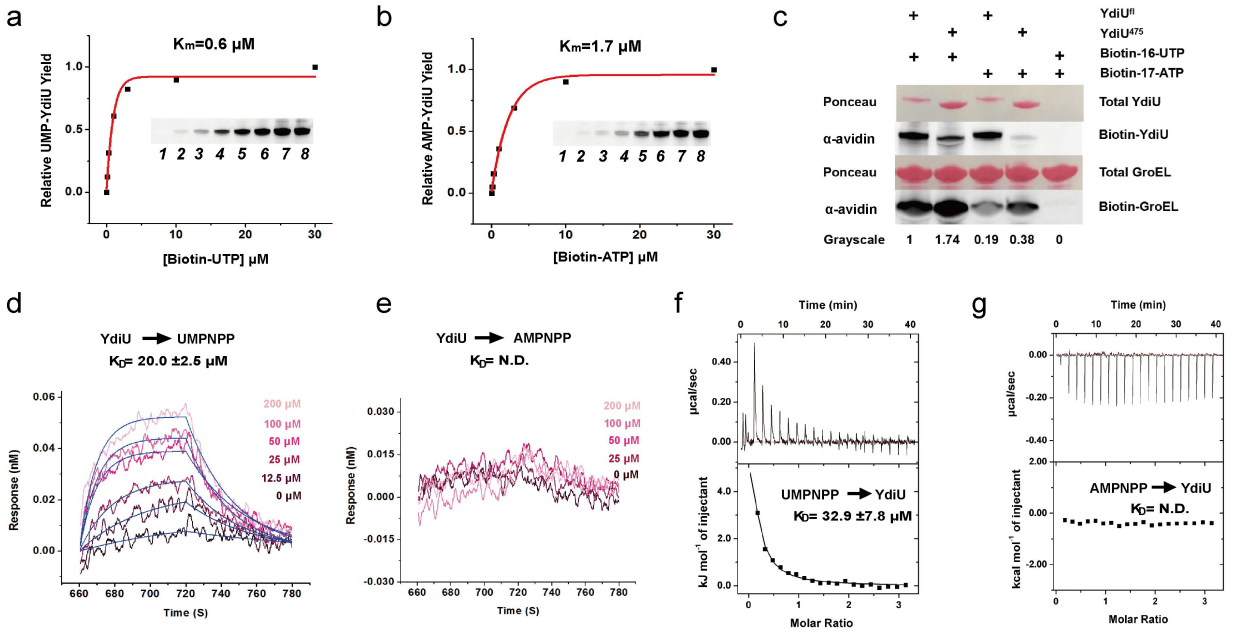

Fig.4. YdiU prefers UTP over ATP as co-substrate.

(a-b) The K_m values of UTP or ATP as catalyzed by YdiU were determined. Serially gradient diluted Biotin-16-UTP or Biotin-17-ATP was used in the reactions. Lanes 1-8 contained 0 μM, 0.1 μM, 0.3 μM, 1 μM, 3 μM, 10 μM, 30 μM and 100 μM concentrations of the small molecules indicated. Grayscale values of each lane indicate the level of UMPylated YdiU as quantified by Image J software, and enzymatic curves were generated using Origin Pro. (**c**) UMPylation and AMPylation of GroEL catalyzed by $YdiU^{fl}$ and $YdiU^{475}$ in the presence of both $MgCl_2$ and $MnCl_2$. Biotin-16-UTP or Biotin-17-ATP was used as an NMP donor. NMP-modified proteins were detected by avidin blotting. Total proteins were visualized by Ponceau S staining of the blot before blocking. The grayscale values of UMP-GroEL in each lane were quantified using the Image J software (**d-e**) The affinity between YdiU and UTP or ATP analog was detected by bio-layer interferometry (BLI). BLI experiments were performed by loading YdiU onto a super streptavidin biosensor and then adding to different concentrations of UMPNPP and AMPNPP. The dissociation constant (K_D) values with the corresponding standard deviations and the R2 values of the fits were obtained by steady state analysis. (**f-g**) ITC titration of YdiU with UTP or ATP analog. 1.5 mM UMPNPP or AMPNPP was injected into the calorimetric cell containing 0.1 mM YdiU. The determined KD values are indicated.

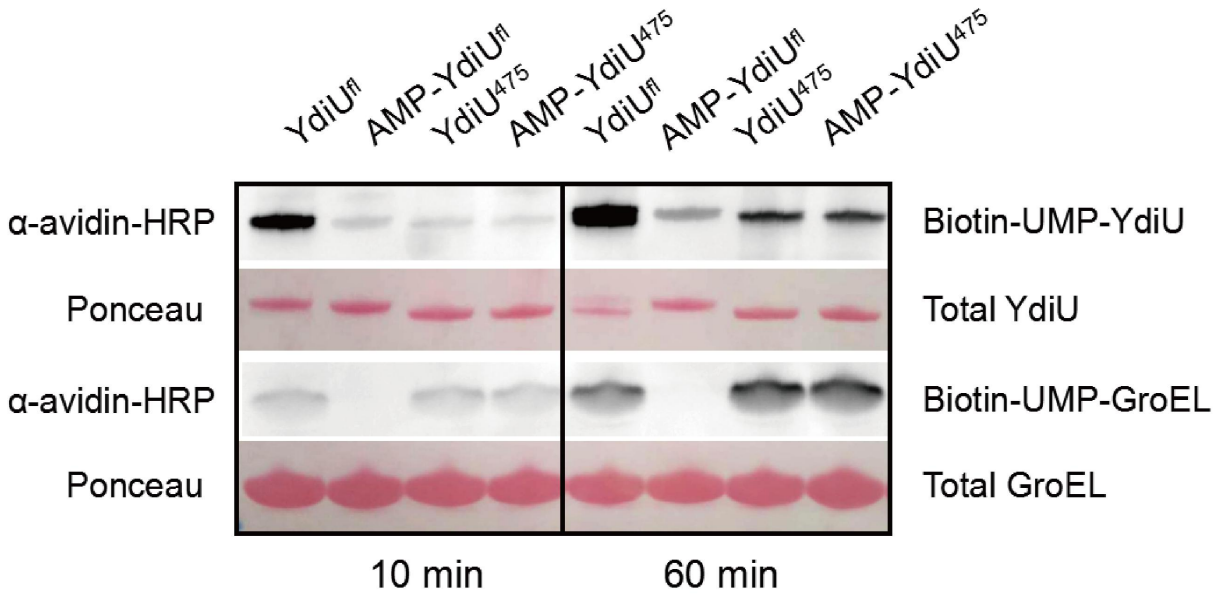

Fig.5. Self-AMPylation inhibits UMPylation activity of YdiU.

$YdiU^{fl}$ and $YdiU^{475}$ were AMPylated *in vitro* and purified. Then UMPylation activities to substrate GroEL were detected using biotin-based avidin blotting. Un-AMPylated $YdiU^{fl}$ and $YdiU^{475}$were used as control. Total proteins were visualized by Ponceau S staining of the blot before blocking.

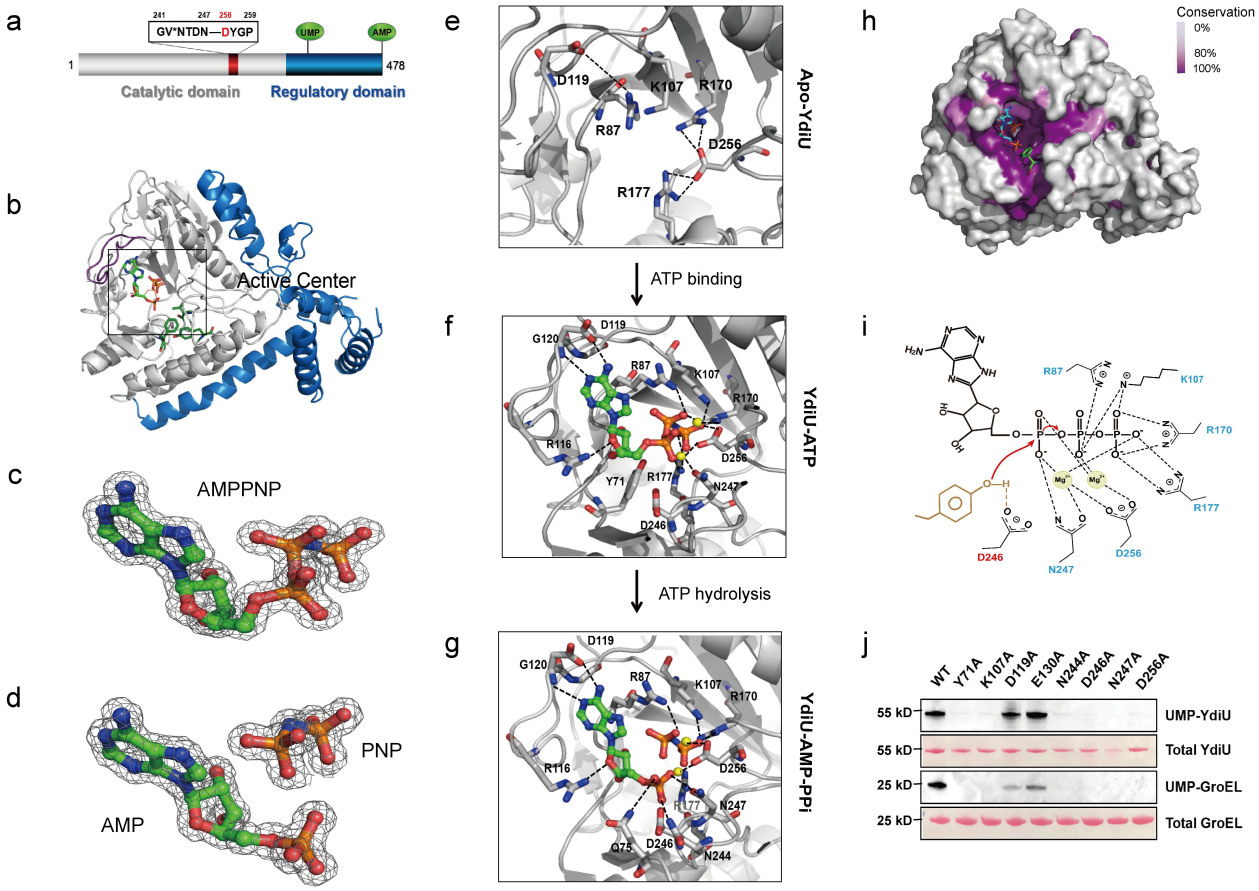

Fig.6. Structural insight into the catalytic mechanism of YdiU-mediated NMPylation.

(**a**) Schematic representation of the domain architecture of YdiU. The conserved catalysis motif and the major self-UMPylation/self-AMPylation sites are highlighted. (**b**) Overall structure of YdiU is shown as a cartoon. The loop from Lys107 to Arg121 responsible for the basic fixing is highlighted by purple. The active center is marked by a black frame. (**c-d**) Well defined electron density maps of AMPPNP and AMP-PPi from YdiU-AMPNPP complex and YdiU-AMP-PPi complex respectively. The 2Fo-Fc omit electron densities are contoured at 2.0 σ. The AMPNPP and AMP-PPi are shown in stick mode. (**e-g**) Zoomed view of the active sites of Apo-YdiU, YdiU-AMPNPP and YdiU-AMP-PPi. Overall structure of YdiU is shown in cartoon and the key residues are highlighted by sticks. Hydrogen bonding interactions between residues of YdiU or YdiU and nucleotide are all indicated as black dashed lines. (**h**) Sequence conservation of YdiU among species. Overall structure of YdiU is shown in surface mode. Highly conserved residues are colored in purple and less conserved ones are colored in light grey. Substrate Tyr is docked into the predicted substrate-binding site and shown in stick. (**i**) The proposed mechanism of

YdiU-mediated NMPylation. The β and ɤ phosphates are stabilized by four positively charged residues, and the two Mg^{2+}. Mg^{2+} are further fixed by Asp256 and Asn247. Asp 246 acts as the general base and activates the oxygen of the hydroxyl group from Tyr or the nitrogen from His for nucleophilic attack. (**j**) UMPylation activity of YdiU mutants with Biotin-16-UTP, as detected by streptavidin HRP blot. Total proteins were visualized by Ponceau S staining of the blot before blocking.

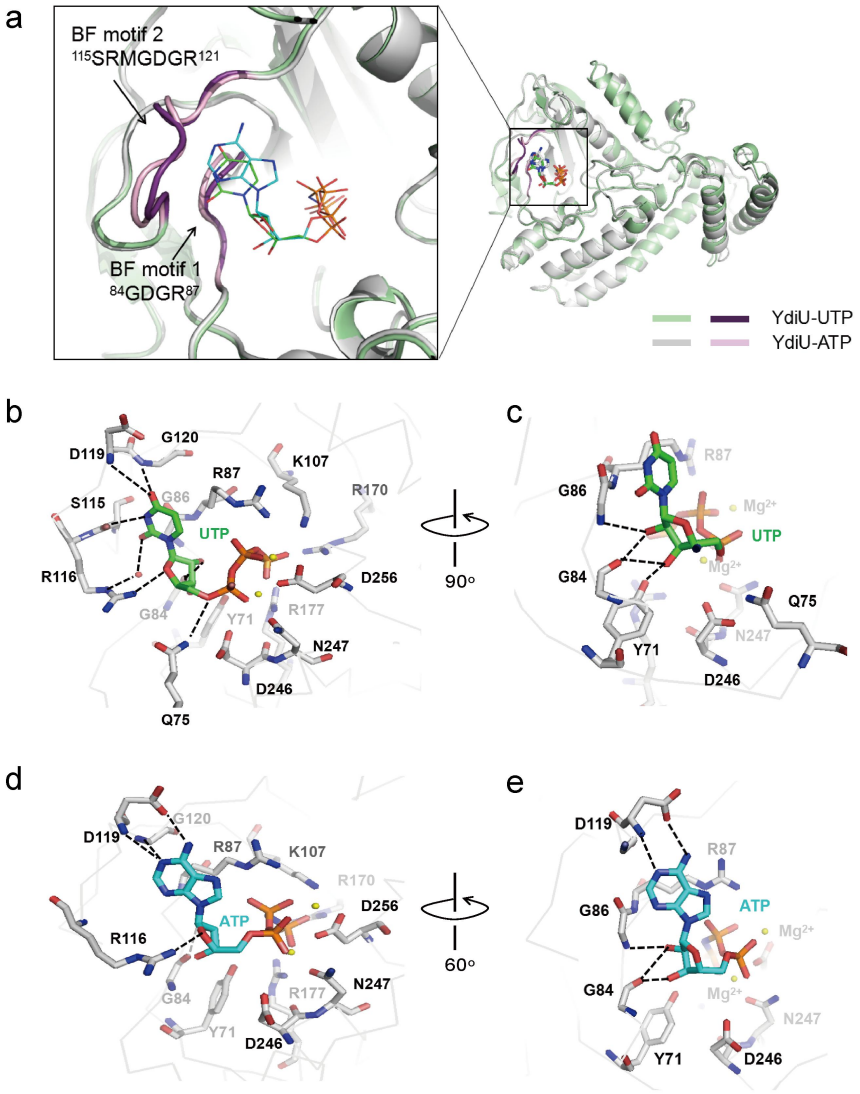

Fig.7. Structural basis for the nucleiotide preference of YdiU.

(**a**) The superimposition of crystal structure of YdiU-AMPPNP and model of YdiU-UTP via molecular docking is colored as indicated. A close-up view shows that two conserved loops (BF motif 1 and BF motif 2) shift towards each other upon ATP and UTP binding. (**b-c**) Hydrogen-bonding network between UTP and YdiU. Related residues are shown in sticks, water molecule is shown as a red sphere, and hydrogen bonds are all indicated as black dashed lines. (**d-e**) Hydrogen-bonding network between ATP and YdiU. Related residues are shown in sticks and hydrogen bonds are all indicated as black dashed lines.

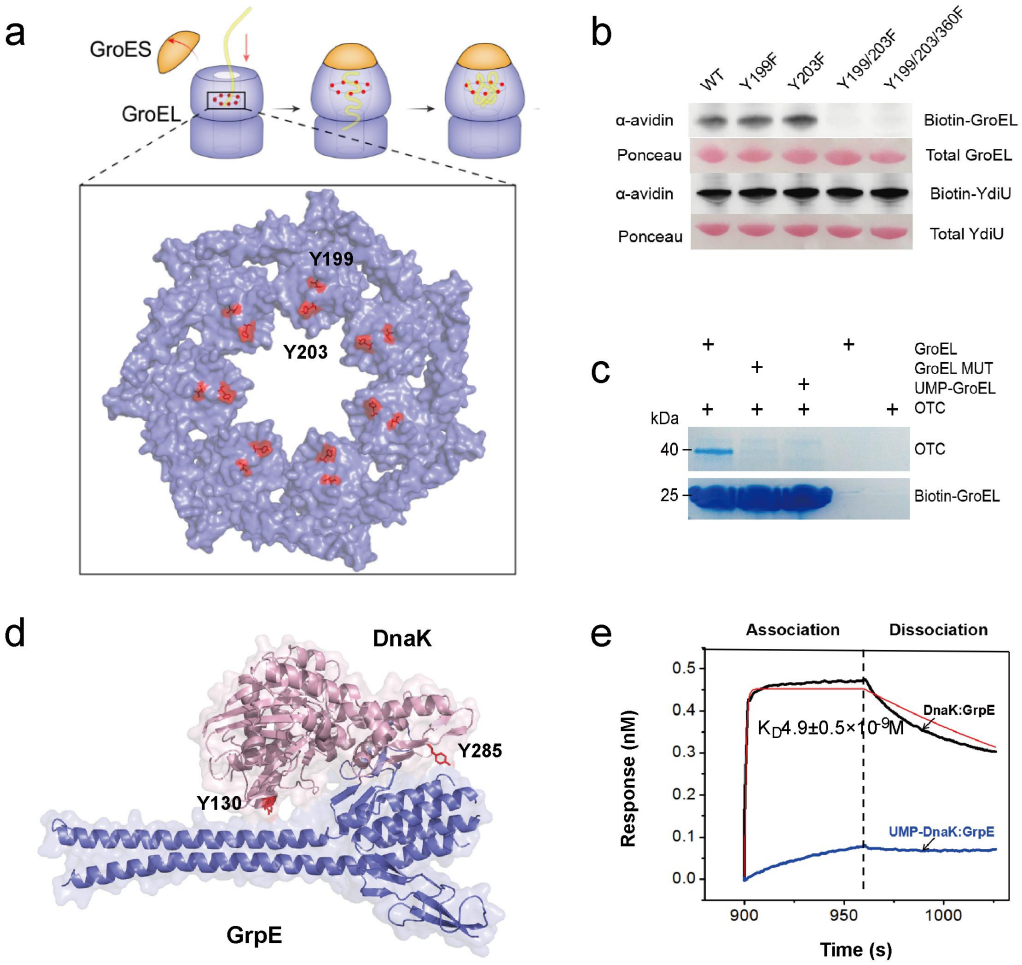

Fig.8. UMPylation of GroEL and DnaK prevents their binding substrates or co-factors.

(**a**) Structural presentation shows that Y199 and Y203 of GroEL are located in the hydrophobic pore important for substrate binding. Both Y199 and Y203 are highlighted as red sticks. PDB code:2CGT. (**b**) The Y199F/Y203F double mutant could not be UMPylated by YdiU, suggesting Y199 and Y203 are the major *in vitro* UMPylated sites of GroEL. The UMPylation reactions were performed with Biotin-16-UTP and $MnCl_2$ followed by avidin blotting. Total proteins were visualized by Ponceau S staining of the blot before blocking. (**c**) UMPylation of GroEL impairs substrates binding. The interaction between UMP-GroEL and substrate OTC was detected by an improved streptavidin pull-down assay, see also Supplementary Fig.S9. (**d**) Y285 and Y130 are located in the interaction surface between DnaK and GrpE. Y285 and Y130 are highlighted as red sticks. PDB code: 1DKG. (**e**) UMPylation of DnaK inhibits DnaK from binding co-factor GrpE. The affinities of native DnaK or UMP-DnaK and GrpE were measured by bio-layer interferometry, see also Supplementary Fig.S11.

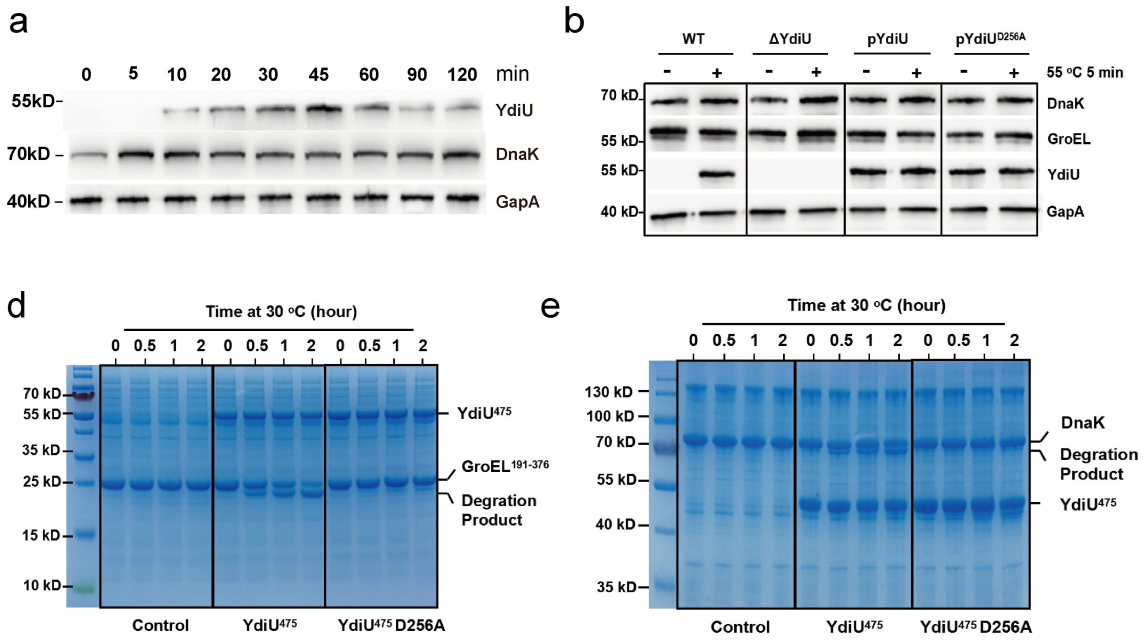

Fig.9. YdiU-mediated UMPylation promotes the degradations of chaperones.

(a) At the indicated time points after heat treatment (55°C, 2min), The expression levels of YdiU and DnaK of WT *Salmonella* were quantified by western blot. GapA (also known as GADPH) was used as a loading control. (**b**) The levels of DnaK, GroEL and YdiU of four *Salmonella* strains with or without heat treatment (55°C, 5min). GapA (also known as GADPH) was used as a loading control. (**d-e**) *In vitro* degradation of chaperones. GroEL$^{191\text{-}376aa}$ and DnaK were expressed in *E.coli* BL21 (DE3) ΔYdiU strain. After sonication and centrifugation, YdiU^{475aa} or YdiU^{475aa} D256A was added into the samples at a final concentration of 5mg/ml and incubated at 30 °C for the indicated time. Then the aliquots were mixed with 2× SDS loading buffer, analyzed using 12.5% SDS-PAGE gel, and stained with Coomassie brilliant blue.

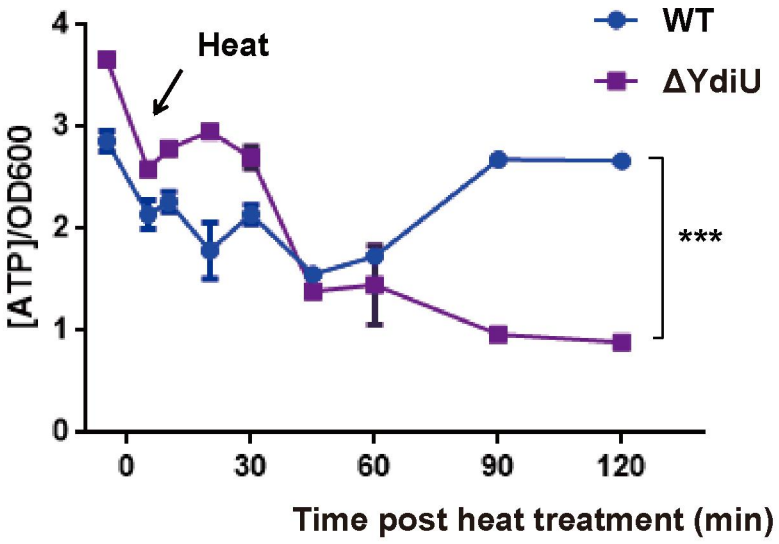

Fig.10. YdiU prevents *Salmonella* from stress-induced ATP depletion.

ATP levels of WT *Salmonella* and ΔYdiU during recovery from heat injury. All experiments were performed as three repeats and the mean values and error bar are presented. The average amount of intracellular ATP was obtained by calculating the ratio of total ATP and OD600. Statistical significance is indicated by ***$P < 0.001$ using a t-test.

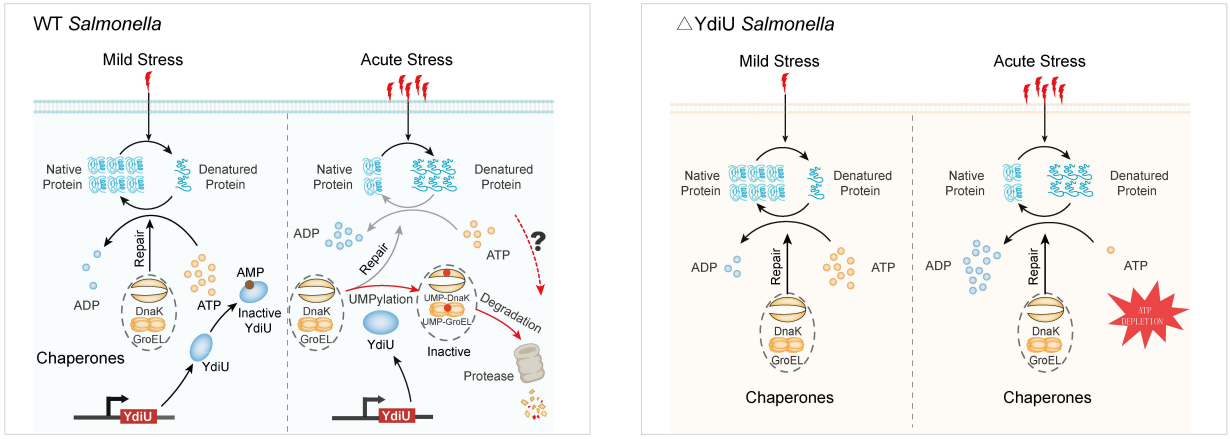

Fig.11. The model of YdiU-mediated chaperone-protease switch during acute heat stress.

i). Under mild stress, only a fraction of proteins are denatured. Chaperones repair misfolded proteins using a small amount of ATP. The intracellular ATP remains in a relatively high level. At that time, even though YdiU is expressed, it will exist in a self-AMPylated and inactive state. Thus, little difference is observed in the survival ability of WT and ΔYdiU under mild stress condition. ii). Under acute stress, a mass of proteins are denatured, the repairment mediated by chaperones consumes lots of ATP. Under ATP-limited condition, YdiU is activated as an UMPylator. Then, YdiU will inactive chaperones through UMPylation and promote their degradation. The degradation of other UMPylated substrates of YdiU might be promoted as well. As a result, bacteria will switch from chaperone-mediated repairment to protease-mediated self-protection and keep sufficient energy for survival. The YdiU knockout strain will die of ATP depletion causing by excessive ATP consumption of chaperones under acute stress.